


Review

AIEgen-Based Nanomaterials for Bacterial Imaging and Antimicrobial Applications: Recent Advances and Perspectives

Zipeng Shen ¹, Yinzhen Pan ¹, Dingyuan Yan ¹, Dong Wang ^{1,*}  and Ben Zhong Tang ^{2,*}

¹ Center for AIE Research, Shenzhen Key Laboratory of Polymer Science and Technology, Guangdong Research Center for Interfacial Engineering of Functional Materials, College of Materials Science and Engineering, Shenzhen University, Shenzhen 518060, China

² Shenzhen Institute of Molecular Aggregate Science and Engineering, School of Science and Engineering, The Chinese University of Hong Kong, Shenzhen 518172, China

* Correspondence: wangd@szu.edu.cn (D.W.); tangbenz@cuhk.edu.cn (B.Z.T.)

Abstract: Microbial infections have always been a thorny problem. Multi-drug resistant (MDR) bacterial infections rendered the antibiotics commonly used in clinical treatment helpless. Nanomaterials based on aggregation-induced emission luminogens (AIEgens) recently made great progress in the fight against microbial infections. As a family of photosensitive antimicrobial materials, AIEgens enable the fluorescent tracing of microorganisms and the production of reactive oxygen (ROS) and/or heat upon light irradiation for photodynamic and photothermal treatments targeting microorganisms. The novel nanomaterials constructed by combining polymers, antibiotics, metal complexes, peptides, and other materials retain the excellent antimicrobial properties of AIEgens while giving other materials excellent properties, further enhancing the antimicrobial effect of the material. This paper reviews the research progress of AIEgen-based nanomaterials in the field of antimicrobial activity, focusing on the materials' preparation and their related antimicrobial strategies. Finally, it concludes with an outlook on some of the problems and challenges still facing the field.

Keywords: aggregation-induced emission; nanomaterials; antimicrobial; multi-drug resistant



Citation: Shen, Z.; Pan, Y.; Yan, D.; Wang, D.; Tang, B.Z. AIEgen-Based Nanomaterials for Bacterial Imaging and Antimicrobial Applications: Recent Advances and Perspectives. *Molecules* **2023**, *28*, 2863. <https://doi.org/10.3390/molecules28062863>

Academic Editors: Mingdi Yan and Már Måsson

Received: 31 January 2023

Revised: 14 March 2023

Accepted: 16 March 2023

Published: 22 March 2023



Copyright: © 2023 by the authors. Licensee MDPI, Basel, Switzerland. This article is an open access article distributed under the terms and conditions of the Creative Commons Attribution (CC BY) license (<https://creativecommons.org/licenses/by/4.0/>).

1. Introduction

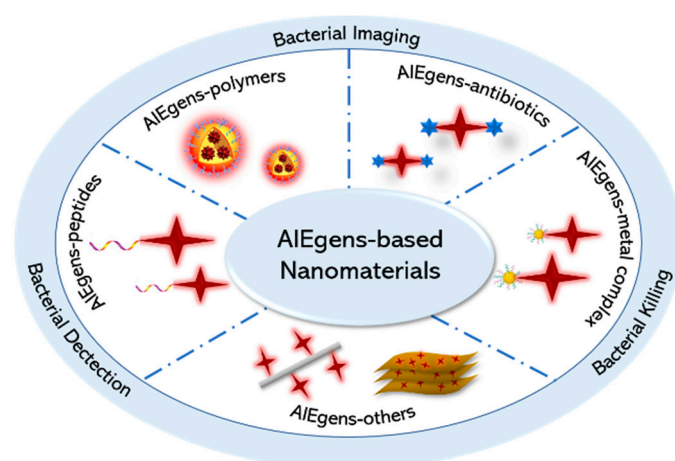
Bacterial infections have long been a severe issue in clinical treatment [1] that can lead to serious complications (sepsis, skin disease, endocarditis, meningitis, pneumonia, etc.) and even threaten life [2–4]. Bacterial infections have been effectively controlled since 1928, when penicillin (the first antibiotic, followed by many others) was invented [5]. However, due to the overuse and misuse of antibiotics, antimicrobial resistance (AMR) is becoming more serious [6–8]. According to the World Health Organization (WHO), around 700,000 people worldwide die from multi-drug resistant (MDR) bacterial infections every year, and the number could reach 10 million by 2050 [9–11]. Because developing antibiotics against MDR bacterial infections is time and energy consuming, the rate of antibiotic development can hardly keep up with the rate of production of MDR bacterial infections. Therefore, there is an urgent need to develop a new alternative antibacterial strategy that not only has good broad-spectrum antibacterial activity, but also avoids the development of resistance as much as possible.

Biomedical materials developed rapidly over the last decade. Antimicrobial therapy based on nanomaterials is considered to be a promising antimicrobial strategy [12]. It mainly includes antibacterial polymers [13–16], photothermal therapy (PTT) [17–19], photodynamic therapy (PDT) [20–23], the specific delivery and stimulation-triggered release of antibiotics based on nanomaterials [24–26], catalytic killing of bacteria and anti-virulence therapy based on nanoenzymes [27], etc. In contrast to single materials, nanomaterials can be integrated with a variety of different antibacterial materials to build nanoscale diagnostic

and therapeutic platforms and realize multi-pronged antimicrobial strategies for efficient and broad-spectrum antimicrobial therapy.

Antibacterial nanomaterials based on aggregation-induced emission luminogens (AIEgens) have received a lot of attention recently [28–30]. As a fluorescent material, AIEgens can be used for fluorescence imaging for microorganisms [31–35]. Existing detection methods, such as polymerase chain reaction (PCR), DNA microarrays [36], targeted specific immunoassay [37], mass spectrometry [38], and surface-enhanced Raman spectroscopy [39], are time-consuming, less accurate, and difficult to operate [40]. The use of AIEgens not only avoids the aggregation-caused quenching (ACQ) effect of traditional photosensitizers [41–43], but it also provides a good imaging tracer for bacteria, allows for real-time, dynamic observation of the interaction process between nanomaterials and bacteria, and reveals the antibacterial mechanisms of materials [44,45], which all benefit from AIEgens' low background, high signal-to-noise ratio, and non-invasive real-time imaging [46–48]. On the other hand, AIEgens, as photosensitizers, enable photodynamic and photothermal treatment of pathogenic microorganisms. AIEgens can not only achieve long-wavelength excitation and emission through the regulation of molecular structures, but also achieve combined photodynamic and photothermal therapy for bacterial infections through the regulation of energy levels. Compared with traditional antibiotics, this antibacterial method offers good broad-spectrum antibacterial activity, and it does not easily produce drug resistance. In addition, compared with heavy metal ions, AIEgen, as an organic material, has less cytotoxicity and better biocompatibility. Phototherapy, as a non-invasive technique with high spatial and temporal accuracy, attracted wide attention in the field of antibacterials [49]. AIE-active photosensitizers can not only kill pathogens but also act as immune effector molecules to initiate and regulate the host's immune defence system [50–52]. Therefore, AIEgens can effectively recognize and inhibit bacterial growth and reduce bacterial drug resistance under imaging guidance [53].

Inspired by this, we focused on recent research advances in the antimicrobial domain based on AIEgen-based nanomaterials and introduced some new antimicrobial nanomaterials and antimicrobial strategies. In this review, we focus on a number of nanotherapeutic systems constructed by AIEgens with polymers, antibiotics, metal complexes, and peptides as well as some of the novel antibacterial therapeutic strategies involved (Scheme 1). Finally, it is hoped that the review of this paper will inspire more intensive research in the new frontier field of antibacterial nanomaterials.



Scheme 1. Schematic diagram of the representative AIEgen-based nanomaterials.

2. Nanomaterials with AIEgens—Polymers for Antimicrobial Application

AIEgens were proven to have good bactericidal effects against various microorganisms in recent years [54–57]. Although small molecules alone are beneficial for photodynamic therapy of bacteria, their photostability is relatively poor compared to polymers; thus, the development of polymer-based AIEgens is highly necessary. Some commonly used

methods mainly cover drugs or target molecules and the self-assembly of polymers to build a nano-assembly system to achieve multifunctional requirements. Porous, hollow, polymeric capsules and amphiphilic polymers are commonly used materials in these assembly systems [58,59]. Recently, Huang et al. [60] designed a polymer-based NIR-II AIEgen PDTPTBT, which was then encapsulated with liposomes into a nanomaterial (L-PDTPTBT) to improve the dispersion and biocompatibility of the material, as shown in Figure 1a. In vitro experiments demonstrated that L-PDTPTBT has excellent photothermal conversion effects under 808 nm laser irradiation, with the highest temperature reaching 55 °C, which can easily destroy the structure of the bacterial membrane and kill bacteria (Figure 1b,c). Subsequent in vivo experiments further revealed that L-PDTPTBT had an excellent bactericidal effect on both diabetic wound infections and subcutaneous bacterial infections, and the number of bacteria was significantly reduced (Figure 1d,e).

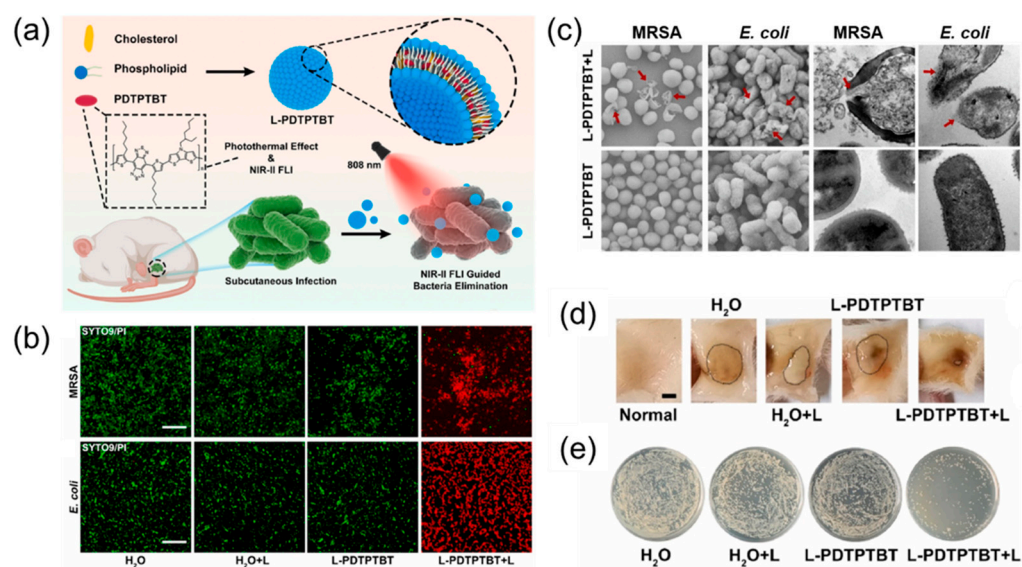


Figure 1. (a) Schematic illustration of nanofabrication of L-PDTPTBT and its application in photothermal therapy of bacterial infection. (b) Live (SYTO 9)/dead (PI) staining of MRSA and *E. coli* after different treatments. Scale bar: 20 μ m. (c) Morphology changes and leakage of cytoplasm of MRSA and *E. coli* bacteria after different treatments, characterized by SEM and TEM. (d) Images of subcutaneous tissues seven days after different treatments. Scale bar: 2 mm. (e) Representative LB agar of *E. coli* bacterial colonies harvested from subcutaneous abscesses seven days after different treatments ($n = 5$). Adapted from [60], copyright 2022, Elsevier Ltd.

Polymer-based AIE molecules do have excellent photostability, but the degradation performance of the polymer is also a concern [61]. As an antibacterial drug, it is necessary not only to have good antibacterial properties, but also to minimize the biological toxicity of the drug. This requires antibiotics to degrade metabolism well in the human body and to reduce the amount of time retained in the body. Based on this, Chen et al. [62] designed a novel antimicrobial polymer with ester bonds connecting the polymeric backbone and functional segments and then cleverly introduced AIEgens into the polymer system to successfully enable the imaging and killing of bacteria (Figure 2a). The cationic amino segments of the polymer backbone can interact with the negatively charged bacterial membrane and destroy the integrity of the membrane. The lipophilic alkane segments can be inserted into the bacterial membrane, causing a distortion of the bacterial membrane structure that promotes its destruction and accelerates the death of the bacteria. The introduction of ester bonds can give antimicrobial drugs good antibacterial activity in the short term. In the biological environment, they degrade well due to the hydrolysis of lipases, thereby reducing the harm to the body. Subsequent experimental results also show that the antibacterial rate of Q-PGEDA-OP/TPE system on AMO^r *S. aureus* (Figure 2c) and

AMO^r *E. coli* (Figure 2d) was more than 99%, and the subsequent SEM results show that the membrane structure of the bacteria was significantly damaged (Figure 2e).

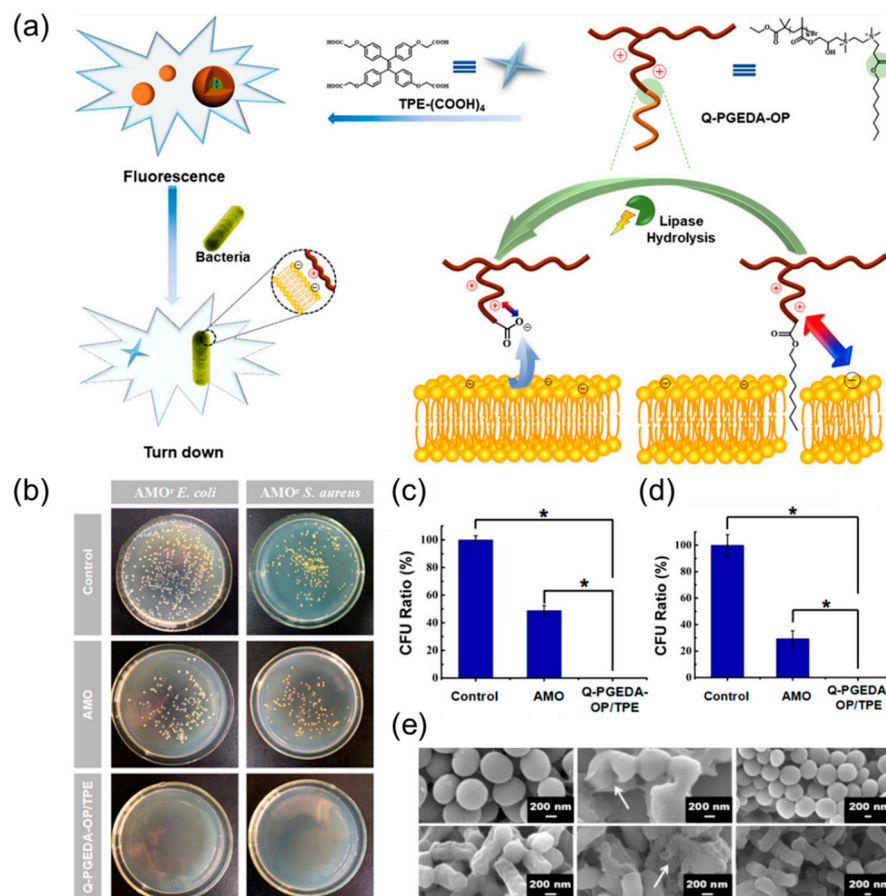


Figure 2. (a) Schematic illustration of tailoring the well-defined polymeric Q-PGEDA-OP/TPE antimicrobial system for the bacterial detection and the antibacterial activity of the Q-PGEDA-OP prior to and after hydrolysis. (b) Photographs of colony-forming units (CFU) for AMO^r *S. aureus* and AMO^r *E. coli* treated with AMO or Q-PGEDA-OP/TPE on the LB agar plate; CFU ratio of (c) AMO^r *S. aureus* and (d) AMO^r *E. coli*. Note: Asterisk (*) indicates significant differences ($p < 0.05$) between every two groups. (e) SEM images of AMO^r *S. aureus* and AMO^r *E. coli* treated with PBS, Q-PGEDA-OP, and Q-PGEDA-COOH. Adapted from [62], copyright 2018, American Chemical Society.

3. Nanomaterials with AIEgen—Antibiotics for Antimicrobial Application

There is no doubt that antibiotics have made remarkable progress in treating bacterial infections since 1928 [63,64]. However, with the overuse of antibiotics and the abuse of broad-spectrum antibiotics, the number of infections caused by MDR bacteria has increased dramatically in recent years [65]. In addition, intracellular bacteria are one of the deadliest causes of drug resistance. After being ingested by phagocytes, the bacteria can escape from the endosomes and proliferate in the cytoplasm [66]. In addition, it is difficult for most antibiotics to play a bactericidal role due to their poor cellular penetration and short intracellular retention time [67]. Thus, how to deliver antibiotics exactly to the site of bacterial infection is important. The emergence of biodegradable nanomaterials has solved this problem well. Currently, commonly used nanomaterials such as liposomes, nanoparticles, and micelles are widely used for the intracellular delivery of antibiotics [68].

Studies have shown that macrophages infected with intracellular bacteria produce a number of different intracellular signals, such as the high expression of various enzymes by intracellular bacteria such as lipase, phosphatase, and phospholipase [69,70]. In addition, cationic polypeptides, hydrophobic carbon chains, and ferric carrier chelates were shown to enhance the ability to target bacteria [71,72]. Based on this, Chen et al. [73]

designed a nanomaterial, mPET@D_{Fe}C, that enables macrophage targeting, intracellular bacteria that trigger drug release, and real-time fluorescence monitoring. First, the AIE fragment was introduced into the polymeric carrier Man-g-P(EPE-r-TPE) via copolymerization, and then ciprofloxacin (CIP) and deferoxamine (DFO) were connected to obtain the siderophore–antibiotic conjugate D_{Fe}C (improve the targeting of intracellular bacteria). Then, Man-g-P(EPE-r-TPE) and D_{Fe}C were self-assembled to obtain the final nanoparticles of mPET@D_{Fe}C. Because there is a fluorescence resonance energy transfer (FRET) effect between the polymer carrier containing the AIE fragment and the drug iron carrier conjugate, the drug release process can be monitored in real time through changes in the fluorescence emissions of the nanoparticles (Figure 3a). Second, mPET@D_{Fe}C can effectively enter macrophages through mannose-mediated endocytosis and then achieve polymer degradation and D_{Fe}C release under the action of lipase and phospholipase secreted by intracellular bacteria with strong specificity and no damage to normal macrophages (Figure 3b). Finally, when D_{Fe}C is ingested by bacteria to realize sterilization, the FRET effect is stopped and the AIE effect is restored, thereby realizing the fluorescence monitoring of intracellular bacteria (Figure 3b).

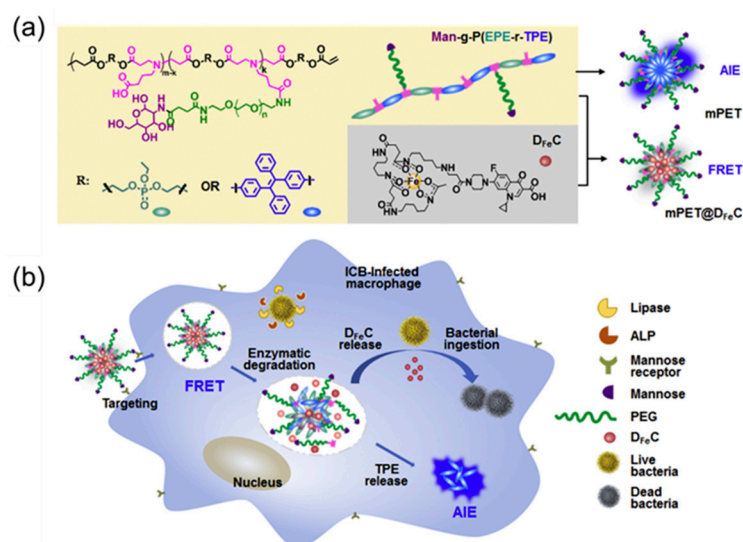


Figure 3. (a) Molecular structure of Man-g-P(EPE-r-TPE) and D_{Fe}C and their assembly into mPET and mPET@D_{Fe}C nanoparticles. (b) mPET@D_{Fe}C nanoparticles are internalized into macrophages via mannose-mediated endocytosis, followed by polymer degradation and D_{Fe}C release, which is triggered by the intracellular lipase and phospholipase of infected macrophages. Adapted from [73], copyright 2020, Elsevier Ltd.

In addition to loading drugs through the self-assembly of organic macromolecules, antibiotics can also be loaded with the help of some existing carriers. Organic silica nanoparticles can not only improve the drug loading rate, but also improve the biocompatibility of materials by selecting suitable silica precursors, which are good drug carriers [13,74–76]. Inspired by the guiding role of surfactants in the preparation of nanoparticles, Yan et al. [77] used the AIE molecule MeOTTVP as the framework and adopted the two-template assisted one-pot method to prepare organic silica nanoparticles (AIE-ONs). This nanoparticle can be added to doxorubicin (DOX) to realize the diagnosis and treatment of cancer. Moreover, the antibiotic rifampicin (RF) can be loaded to effectively treat bacterial infections (Figure 4a). Subsequent antibacterial experiments further proved that AIE-ONs can use the MeOTTVP fluorescence of the AIE molecule to achieve targeted imaging of *S. aureus* and *E. coli* (Figure 4b). In addition, under the irradiation of white light, ROS produced by AIE molecules and the loaded drug rifampicin can kill bacteria well, with a bactericidal rate of up to 99.9% (Figure 4c).

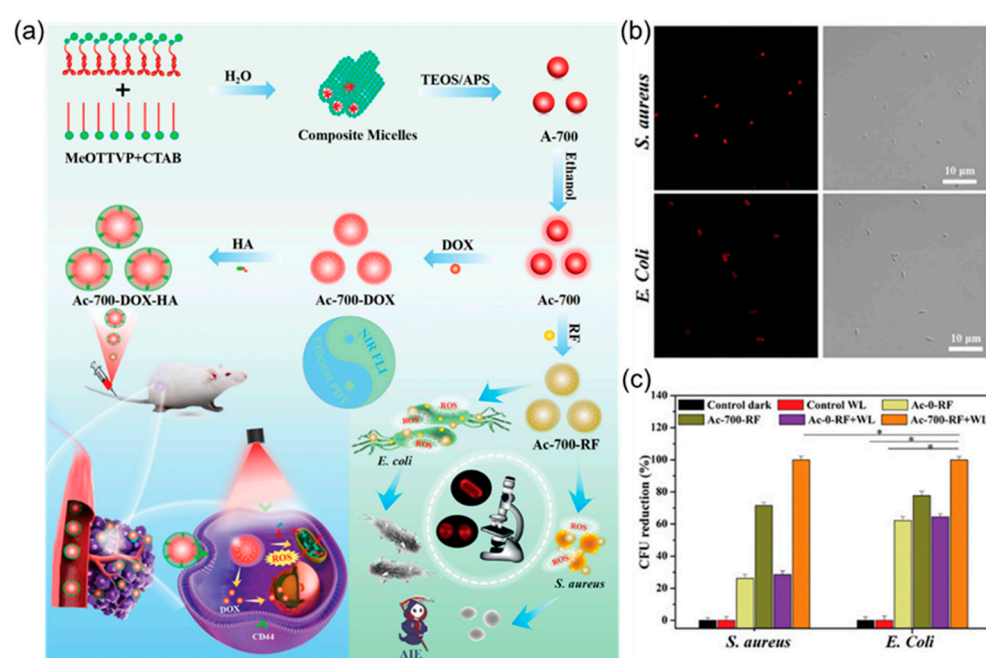


Figure 4. (a) Schematic illustration of the preparing process of AIE-ONs (Ac-700) and their further modifications for efficient theranostic in both tumours and bacteria. (b) CLSM images of *S. aureus* and *E. coli* incubated with Ac-700-RF for 30 min. (c) Colony-forming unit (CFU) reduction of *S. aureus* and *E. coli* treated with Ac-0-RF and Ac-700-RF with/without WL (24 mW cm⁻², 10 min), respectively ($n = 3$, mean \pm SD), *: ($p < 0.05$). Adapted from [77], copyright 2022, Wiley-VCH.

In conclusion, nanomaterials constructed with AIE molecules and antibiotics can greatly improve the therapeutic effects against bacterial infections. It not only avoids the excessive use of antibiotics leading to bacterial resistance, but it also further improves the antibacterial effect of AIE molecules alone, which is a promising therapeutic strategy.

4. Nanomaterials with AIEgen—Peptides for Antimicrobial Application

Antimicrobial peptides are considered to be ideal antimicrobial agents due to their excellent broad-spectrum antibacterial activity and low drug resistance [51,78–80]. Although antimicrobial peptides have good antibacterial effects against both gram-positive and gram-negative bacteria, little is known about their bactericidal mechanisms [81–83]. Therefore, realizing a way to dynamically monitor the interaction between antimicrobial peptides and bacteria is very important [84]. Traditional imaging techniques such as SEM and TEM can only achieve static observation, not dynamic monitoring [85,86]. On the contrary, fluorescence signal monitoring can realize not only dynamic observation but also continuous monitoring [87,88]. The introduction of AIE fluorescent probes can effectively solve this problem. Compared with the fluorescence quenching caused by the aggregation of traditional fluorescent probes, the fluorescence signal of AIE fluorescent probes are significantly enhanced during aggregation, which can allow for good tracer imaging on the target [43].

Based on this, Chen et al. [89] introduced AIE fluorescent probe HBT into antimicrobial peptide HHC36 to obtain the AIE active nanomaterial AMP-2HBT (Figure 5a). Subsequent antibacterial experiments showed that the introduction of AIE fluorescent probes did not damage the antibacterial activity of the antimicrobial peptides, and the growth of *E. coli* was well-inhibited at the concentration of 20 μ M (Figure 5b). In addition, as displayed in Figure 5c, there was a strong green fluorescence signal on the surface of the bacterial membrane, indicating that the antimicrobial peptides mainly adhered to the surface of the bacteria and caused the internal nucleic acid or protein to leak by destroying the structure of the bacterial membranes, thereby leading to the death of the bacteria. In conclusion, the

combination of AIE molecules and antimicrobial peptides not only has a good bactericidal effect, but the process can also be dynamically monitored in real time.

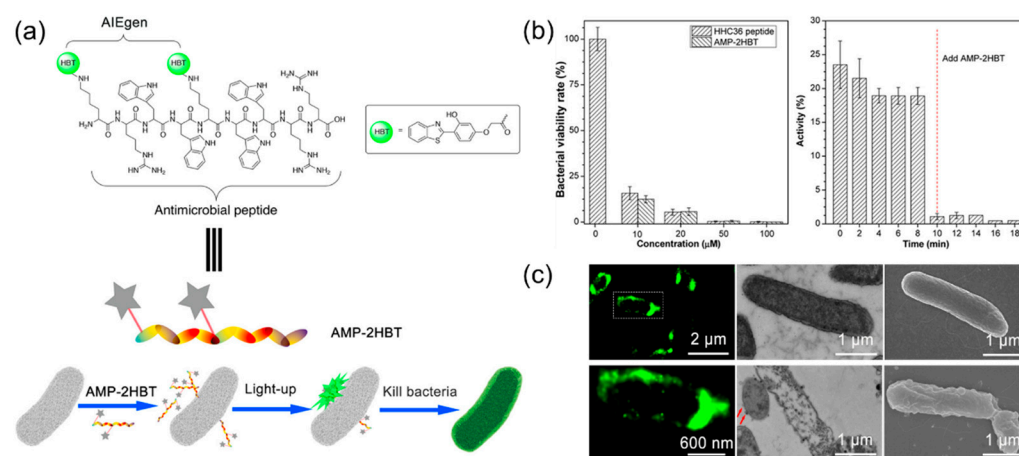


Figure 5. (a) Schematic of AMP-2HBT for bacterial imaging and killing. (b) Left: antimicrobial ability of HHC36 peptide and AMP-2HBT against *E. coli* at different concentrations (0, 10, 20, 50, and 100 μM); right: time-dependent motility of *E. coli* in the presence of AMP-2HBT (20 μM). (c) Fluorescence images of *E. coli* after treatment with AMP-2HBT. The TEM and SEM images of *E. coli* before and after treatment with AMP-2HBT. Adapted from [89], copyright 2018, American Chemical Society.

Compared to external bacterial infections, the treatment of intracellular bacterial infections has always been a difficult problem. The combination of AIE molecules and peptides can not only realize the imaging and sterilization of extracellular bacteria mentioned previously, but it can also have a good effect on the imaging and treatment of intracellular bacterial infections. Qi et al. [90] designed a nano-probe, PyTPE-CRP, specific to casp-1 that can be used for the imaging and treatment of intracellular bacterial infections by taking advantage of the property that macrophages can recognize bacterial infections and induce the activation of casp-1, as shown in Figure 6a. PyTPE-CRP is composed of two parts. As a reactive part, CRP can cleave between amino acids Asp and Ala (red dotted line in Figure 6a) during bacterial infections through the activation of casp-1 enzymes. The resulting PyTPE-CRP residues spontaneously self-assemble into aggregates and accumulate on macrophages containing bacteria. To achieve the specific imaging of bacteria-infected macrophages, AIE fluorophore (PyTPE), in its molecular state, almost does not emit light, but as an aggregate, it shows strong emission, which can realize the imaging and killing of intracellular bacteria. As can be seen in Figure 6b, the fluorescent probes after lysis were evenly distributed around the intracellular bacteria. Under the irradiation of white light, the fluorescent probe after cracking produced a large number of ROS around the bacteria, achieving photodynamic therapy against the bacteria (Figure 6c). At the concentration of 20 μM , it had a good antibacterial effect on *S. aureus*, and the minimum inhibitory concentration was as low as 15 μM (Figure 6d,e).

Most nanomaterials containing antimicrobial peptides kill bacteria directly, mainly by producing ROS, heat, or by disrupting the structure of the bacterial membrane. Recently, a new antimicrobial peptide, HD6, attracted attention [91–93]. Unlike traditional antimicrobial peptides, HD6 traps microbial pathogens through a network of self-assembled fibres, thereby preventing their invasion [94]. Based on this, Fan et al. [95] constructed a bionic analogue peptide, HDMP, which can simulate natural HD6 and achieve the self-assembly process induced by the ligand–receptor interaction to achieve the purpose of bacterial recognition and capture, as shown in Figure 7a. HDMP mainly consists of three parts (Figure 7b). The bacterial targeting recognition part, RLYLRIGRR, can bind to the unique component LTA in Gram-positive bacteria and has specific targeting ability. The peptide skeleton, KLVFF, which mimics the fibre structure in HD6, forms a network of fibres that capture bacteria. The last part is BP, which not only promotes the self-assembly of peptides

into nanoparticles to improve the ability of intravenous drug delivery, but it also has the AIE effect, which can monitor the distribution of antimicrobial peptides via fluorescence in real time. From the perspective of antibacterial mechanisms, it first self-assembles into nanoparticles *in vitro* and then binds specifically to bacterial walls, then transforming into a fibre network, triggered by ligand–receptor interaction, to achieve the purpose of capturing and inhibiting bacterial invasion. As can be seen in the SEM photo in Figure 7c, compared with the blank control group, there were many fibre network adhesions on the surface of bacteria in the experimental group, indicating that the HDMP nanomaterials successfully realized the recognition and capture of bacteria. Further *in vivo* infection experiments in mice also demonstrated that HDMP nanomaterials had a good therapeutic effect on *S. aureus* abscesses and bacteraemia.

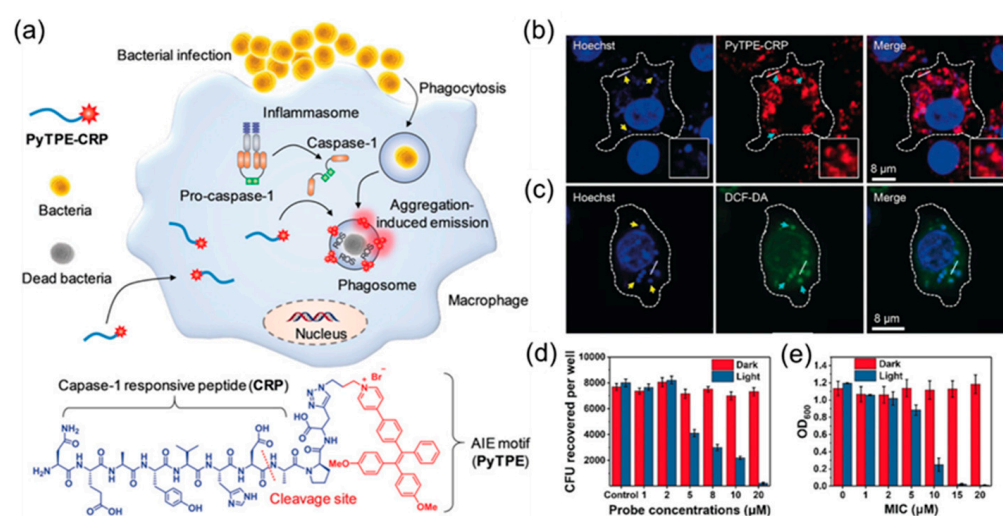


Figure 6. (a) Chemical structures of the molecular structure of PyTPE-CRP and the process of diagnosing and eliminating macrophage-mediated intracellular bacterial infections. (b) Confocal images showing the localization of PyTPE-CRP 60 min after Raw 264.7 macrophages were infected with *S. aureus* (MOI = 20). (c) Confocal images of ROS detection inside the macrophages using DCF-DA after bacterial infection in the presence of PyTPE-CRP. (d) Intracellular survival of *S. aureus* inside Raw 264.7 macrophages in the presence of PyTPE-CRP at different concentrations without and with light irradiation for 10 min at 40 mW cm^{-2} . (e) MIC of PyTPE-CRP towards extracellular *S. aureus* without and with light irradiation (40 mW cm^{-2} , 10 min). Adapted from [90], copyright 2019, Wiley-VCH.

In conclusion, the nanomaterials formed by antimicrobial peptides and AIE molecules not only improve the antibacterial effect of the materials, but also do not easily produce drug resistance. More importantly, the introduction of AIE molecules can give nanomaterials the function of real-time dynamic monitoring, providing a powerful tool for further understanding the antibacterial mechanisms of nanomaterials.

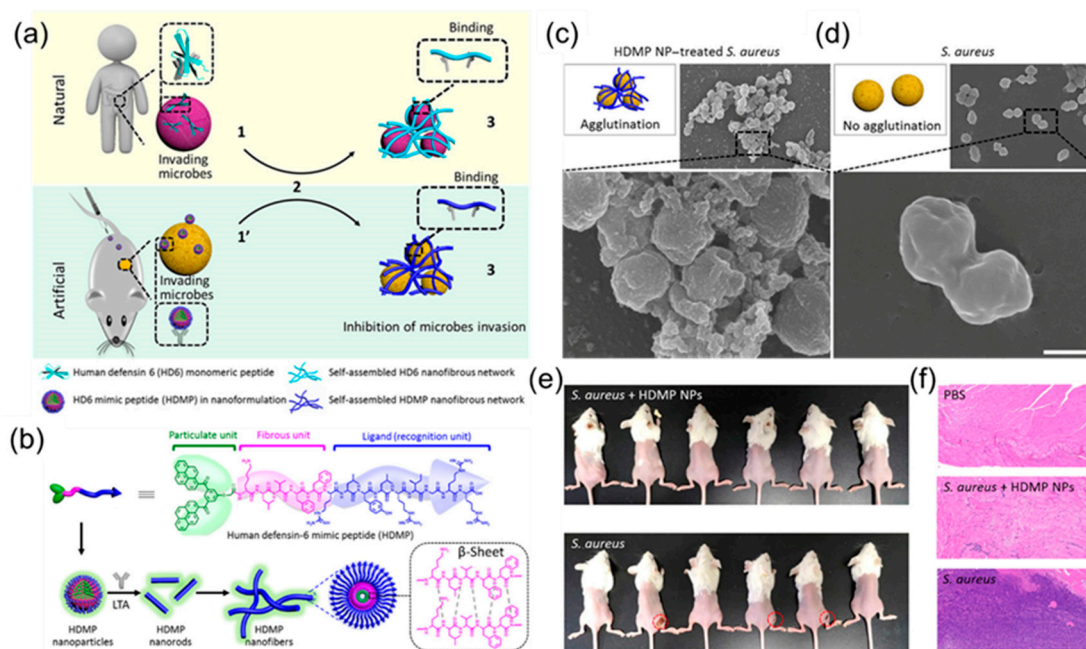


Figure 7. (a) Antimicrobial mechanisms of natural HD6 and artificial HDMP. (b) Schematic illustration of HDMP assembly into nanoparticles, then into nanorods and nanofibers upon the incubation of lipoteichoic acid. Schematic illustrations and SEM images of *S. aureus* treated with (c) HDMP NPs (30 μ M) and bare *S. aureus* (d), indicating that the HDMP NPs transformed into fibrous networks and trapped the *S. aureus*. The SEM images are representative of three independent experiments. Scale bar, 1 μ m. (e) Images of *S. aureus* inoculated in the right leg muscle in mice in the presence and absence of HDMP NPs ($n = 6$). (f) The representative hematoxylin and eosin (H&E) staining images of the leg muscle tissue of mice, indicating that the HDMP NP-treated *S. aureus* did not induce bacterial infection. Adapted from [95], copyright 2020, American Association for the Advancement of Science.

5. Nanomaterials with AIE Metal Complexes for Antimicrobial Applications

Metal-organic frameworks (MOFs) are widely used in drug delivery because of their excellent loading capacity, easy removal, and low biotoxicity [92,96]. More importantly, their adjustable chemistry gives MOFs multiple stimulation–response drug release properties (pH, magnetic field, ions, temperature, and light) to adapt to different physiological environments [96,97].

Based on this, Mao et al. [98] developed a strategy for bacterial detection and treatment by combining MOFs with metabolic labelling technology. First, MIL-100 (Fe) was selected as the carrier of the metabolic marker molecule 3-azide-d-alanine (D -AzAla), which then self-assembled with F-127 to obtain the composite nanomaterial D-AzAla@MIL-100, as shown in Figure 8a. After intravenous injection of D -AzAla@MIL-100, the nanomaterial can be enriched at the site of bacterial infection through the EPR effect. Subsequently, under the action of H_2O_2 secreted by immune cells, MIL-100 (Fe) dissociates and releases D -AzAla, which can then be specifically absorbed by bacteria in the infected area. During this process, unnatural azide groups are expressed on the bacterial wall to achieve bacterial labelling (Figure 8b). Subsequently, selective fluorescent labelling and precise sterilization were achieved via biological orthogonal reactions and PDT with the AIE photosensitizer TPETM (Figure 8c). As shown in Figure 8e, compared to the blank group, mice in the D-AzAla@MIL-100 pretreatment group showed stronger fluorescence images, a longer half-life, and a significantly reduced number of bacteria infected at the wound site (Figure 8e,f).

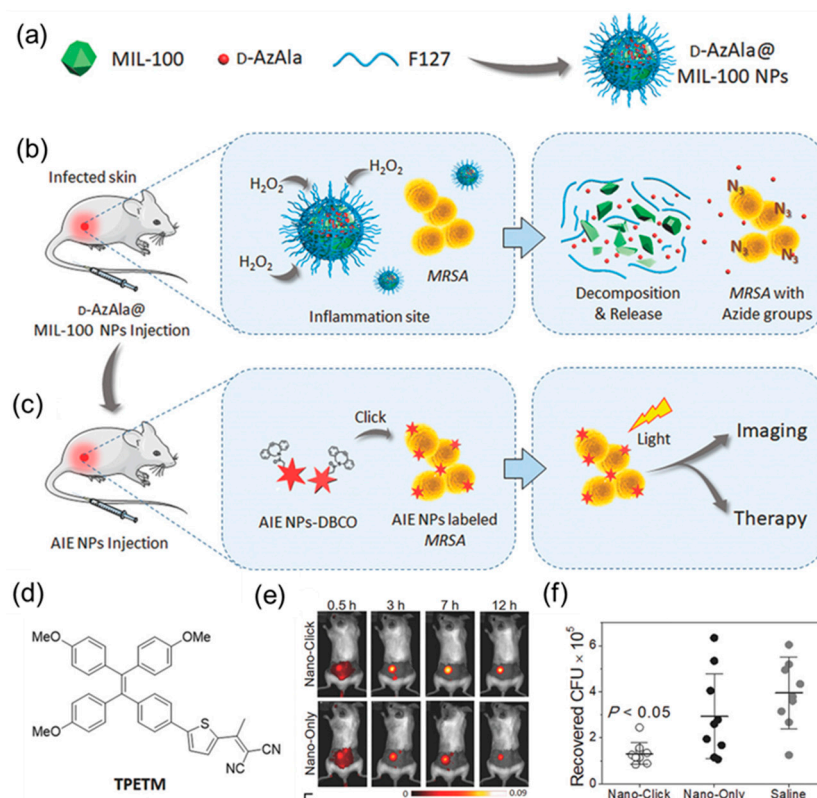


Figure 8. (a) D-AzAla@MIL-100 (Fe) NPs are synthesized by using pluronic F-127 as a matrix to encapsulate the D-AzAla@MIL-100 (Fe). (b) D-AzAla@MIL-100 (Fe) NPs accumulate at the site of the infected tissue and are decomposed in the presence of H₂O₂. (c) Ultrasmall US-TPETM NPs with dibenzocyclooctyne (DBCO) groups bind with bacteria through click reactions, and specific tracking and effective photodynamic therapy (PDT) of bacteria can be achieved in the infected tissue. (d) Chemical structure of TPETM. (e) Time-dependent in vivo fluorescence images of bacteria-bearing mice pretreated with D-AzAla@MIL-100 (Fe) NPs. (f) Bacteria colony-forming unit (CFU) recovered from the infected skin (average \pm the standard error of the mean (SEM)). Adapted from [98], copyright 2018, Wiley-VCH.

In addition, gold nanomaterials are widely used in the biomedical field because of their excellent biocompatibility [99–101]. Notably, when the size of the gold nanomaterials is reduced to the subnanometer scale, these ultra-small Au NCs begin to take on unique physicochemical and biological properties [102]. These properties make Au NCs an excellent candidate for combination therapy with other antimicrobial agents, such as AMPs [103]. Zheng et al. [104] combined the antimicrobial gold nanocluster AuDAMP with the antimicrobial peptide daptomycin Dap to produce a new antimicrobial nanocomplex (Figure 9). The conjugation of gold nanoclusters with AMPs in this compound results in AIE enhancement. The antibacterial mode of Dap mainly occurs through the lipophilic tail inserted into the bacterial cell membrane with the aid of calcium, causing rapid cell membrane damage and potassium ion efflux. Membrane damage encourages the introduction of antimicrobial compounds into the bacteria and leads to more severe bacterial damage at the subcellular level. This strategy provides a new perspective for the synthesis of novel antimicrobial agents and AIE-type fluorescent materials, and it provides a way to further study the specific mechanisms behind the conjugation-induced AIE effect.

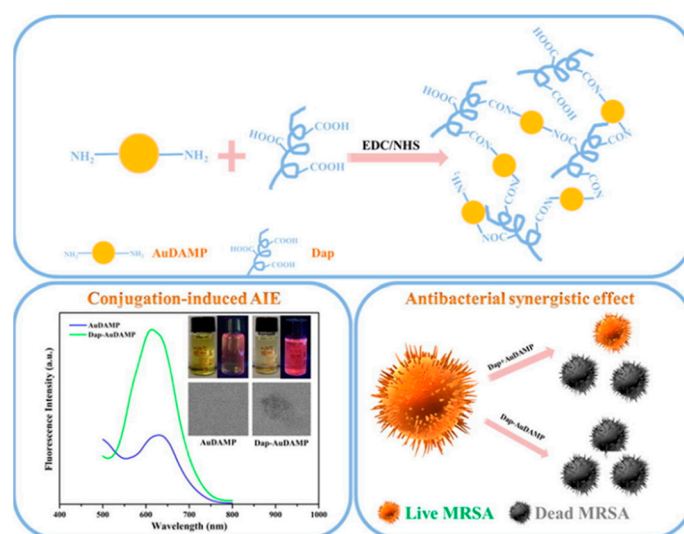


Figure 9. Schematic illustrations of the conjugation strategy for antibacterial Au NCs and Dap, conjugation-induced AIE enhancement, and antibacterial synergistic effects. Adapted from [104], copyright 2019, Elsevier Ltd.

6. Other Nanomaterials with AIEgen for Antimicrobial Applications

On one hand, related diseases caused by bacterial infection seriously threaten human health [98,105–107]; on the other hand, some bacterial communities, such as gut microbes, are essential to human health [91,108]. Therefore, we have pursued improvement of the targeting and killing efficiency of antibacterial agents. Studies have shown that phages are host-specific and can evolve synchronously to infect MDR bacteria [109–111]. However, bacteriophages alone have low antibacterial efficiency, and it is ineffective against acute infections and other severe infectious diseases [112]. In addition, due to the lack of imaging fragments, the target identification, binding, infection, and other processes of phagocytic therapy are not easy to monitor, and it is difficult to evaluate their therapeutic effects in real time.

Therefore, He et al. [113] proposed a novel strategy to bind AIEgens to phages to form a new class of antimicrobial bioconjugates (TVP–PAP) that are used to image and kill specific species of bacteria, as shown in Figure 10a. Not only does this new antimicrobial material retain the specificity of bacteriophage targeting, but the inherent fluorescence of the introduced AIEgens (TVP) also allows real-time monitoring of bacteriophage interactions. At the same time, the highly efficient photodynamic inactivation of TVP and the excellent bacteria-targeting ability of PAP synergistically endow TVP-PAP with excellent bactericidal effects, significantly exceeding the antibacterial effects of the two components individually. As can be seen in Figure 10b, TVP-PAP staining for 30 min can bind well to *P. aeruginosa* (host bacteria) to produce bright fluorescence, and staining efficiency is as high as 100%. However, non-host bacteria *A. baumannii* did not stain all of them, indicating that TVP-PAP can target bacteria accurately. Subsequent antibacterial experiments further proved that TVP-PAP not only has a good bacteria-targeting ability, but it also has a good bactericidal effect on host bacteria, with a selective bactericidal efficiency of up to 90% (Figure 10c,d).

As an inorganic nanomaterial, montmorillonite has been widely used in biomedical fields, such as intestinal diseases, drug delivery, additive manufacturing, and so on [114–118]. Because of its highly ordered lattice arrangement, it has a high cation exchange capacity and surface area; thus, it is a good drug transport carrier [104,119]. In addition, studies show that MMT can absorb bacteria and bacterial enterotoxins well in the body. However, in vitro, its antibacterial effect is very weak [120,121], and it is difficult to meet the needs of clinical external infection treatment with it.

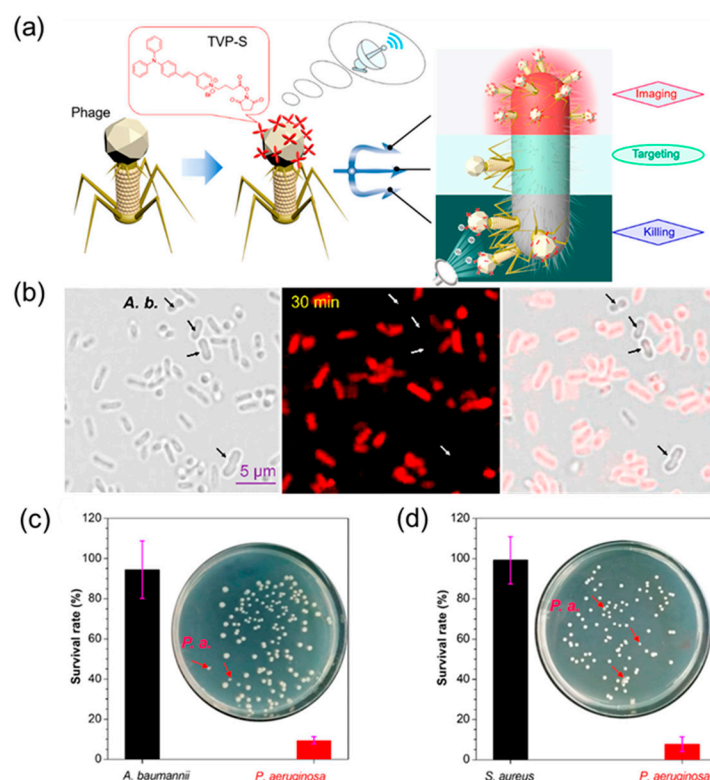


Figure 10. (a) Cartoon illustration of the synergistic effect of AIEgen-modified phages for particularly specific bacterial recognition, real-time fluorescent tracking, phage infection, and synergistic AIE-PDI bacteria-killing activity. (b) Specificity test of TVP-PAP by fluorescence imaging of *P. aeruginosa* and *A. baumannii* coincubated with TVP-PAP. (c) *P. aeruginosa* and (d) *A. baumannii* (each with 1.0×10^5 CFU mL $^{-1}$) incubated together with TVP-PAP (1.59×10^6 PFU mL $^{-1}$). Adapted from [113], copyright 2020, American Chemical Society.

Therefore, Zhang et al. [81] developed an ultra-efficient photodynamic/chemokinetic treatment platform by inserting the aggregation-induced emission (AIE) photosensitizer TPCI into nanolayers of iron-containing montmorillonite (MMT). Here, the introduction of iron atoms can achieve chemodynamic therapy and enhance the effect of photodynamic therapy. Studies show that the site of bacterial infection has a microenvironment with a low pH value and a relatively high endogenous hydrogen peroxide level. Therefore, iron ions can convert the endogenous hydrogen peroxide with low activity into highly toxic hydroxyl radicals under weak acid through the Fenton reaction, thereby inducing bacterial inactivation. Therefore, the TPCI/MMT treatment system can not only carry out efficient PDT through the production of singlet oxygen, but it can also continuously implement CDT by converting endogenous H₂O₂ into highly toxic hydroxyl radicals, as shown in Figure 11a. The generation of hydroxyl radicals and singlet oxygen was subsequently verified with ESR spectroscopy (Figure 11b). The bactericidal effect of TPCI/MMT on *E. coli* and *S. aureus* under white light was more than 99% compared to the blank control group and the group receiving MMT alone (Figure 11c). In addition, it can be seen in the SEM results that TPCI/MMT mainly kills bacteria by destroying the integrity of the bacterial membrane structure (Figure 11d). Subsequently, the antibacterial effect of TPCI/MMT was evaluated with an in vivo infected wound healing assay (Figure 11e). The results showed that TPCI/MMT could effectively promote the healing of infected wounds and significantly reduce the number of bacteria in infected tissues with good therapeutic effects (Figure 11g,h).

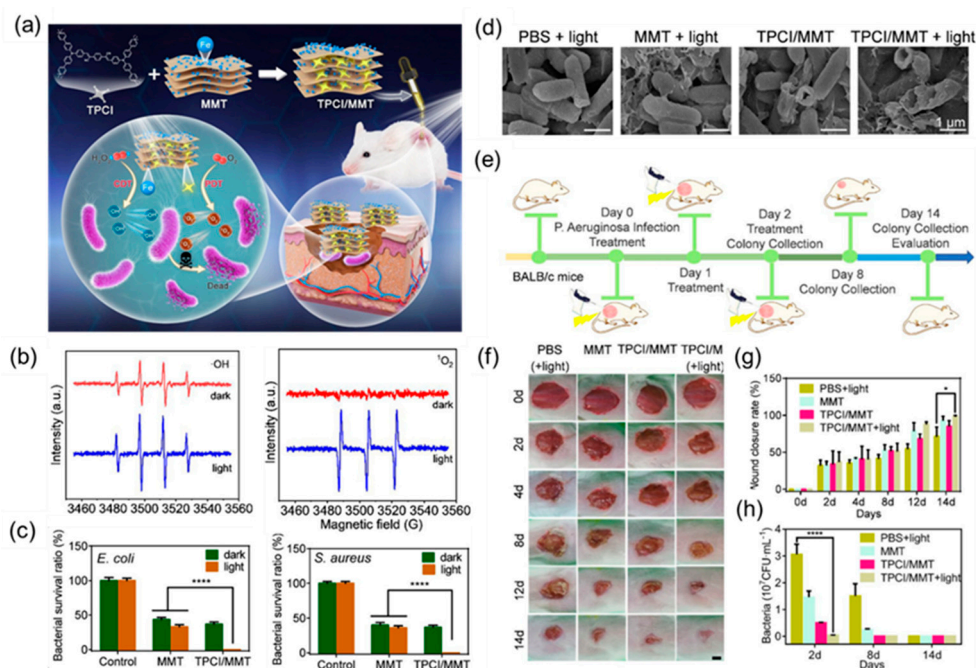


Figure 11. (a) Schematic illustration of the proposed photodynamic/chemodynamic theranostic platform based on TPCI/MMT for efficient bacterial eradication and fast wound healing. (b) ESR spectra of TPCI/MMT for the detection of $\bullet\text{OH}$ (left) and $^1\text{O}_2$ (right) with DMPO before and after illumination. (c) The survival rate of (left) *E. coli* and (right) *S. aureus* treated with MMT ($0.5 \text{ mg}\cdot\text{mL}^{-1}$) and TPCI/MMT ($0.5 \text{ mg}\cdot\text{mL}^{-1}$) with or without light irradiation ($4 \text{ mW}\cdot\text{cm}^{-2}$). (d) SEM images of *E. coli* bacteria treated with PBS, MMT ($0.1 \text{ mg}\cdot\text{mL}^{-1}$), and TPCI/MMT ($0.1 \text{ mg}\cdot\text{mL}^{-1}$). (e) The schematic illustration of drug administration, light treatment, and wound evaluation regimens toward *P. aeruginosa*-infected mice. (f) Representative images of infected skin wounds after various treatments at different time points (0, 2, 4, 8, and 12 days). Scale bar: 50 mm. (g) Assessment of wound healing rate. (h) *P. aeruginosa* bacteria colony removed from the wound area and cultured on LB agar plates; images at days 2, 8, and 14. Adapted from [81], copyright 2022, American Chemical Society.

At present, the regulation of the antibacterial properties of AIE molecules is mainly realized based on the reasonable design of the positively charged molecular framework of AIEgen and specific recognition groups [21,90,122,123]. However, due to their limited molecular skeleton, the further improvement of the antimicrobial properties of AIE molecules is greatly restricted [42]. Here, Guo et al. [124] used AIEgen DTPM as the inner core and prepared a series of AIE nanofibers that could precisely regulate the antibacterial activity by reasonably designing peptides as the recognition system. The preparation process is shown in Figure 12a. First, AIE molecules are coated with amphiphilic molecules to improve the biocompatibility of the materials. Then, the designed peptides are introduced on the surface of AIE molecules via a maleimide–mercaptan addition reaction to regulate the antibacterial activity of nanomaterials. Through mechanism analysis, it was found that this effect can be attributed to the combined action of ROS and antimicrobial peptides produced by AIE molecules, which had obvious synergistic antibacterial effects (Figure 12b). The antimicrobial activity of the materials can be precisely regulated by the modification of different antimicrobial peptides. It can be seen in Figure 12c that K18-modified nanofibers had the best bacterial adsorption effect, followed by K14. In addition, from the bactericidal effect, NFs-K18 also had a very good antibacterial effect (Figure 12d).

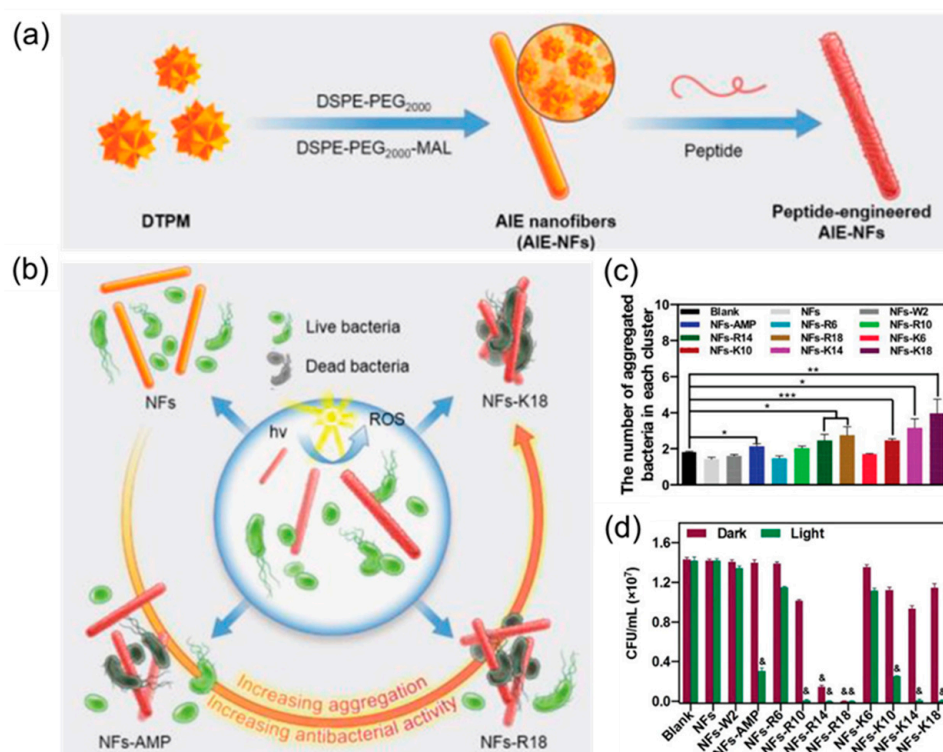


Figure 12. (a) The synthesis of AIE-NFs with different peptides. (b) Schematic illustration of AIE-NFs with different peptides. (c) The number of aggregated *S. aureus* in each cluster. * denotes $p < 0.05$, ** denotes $p < 0.01$, and *** denotes $p < 0.001$. (d) The in vitro antibacterial activity of the indicated AIE-NFs to *S. aureus*. & denotes $p < 0.01$ compared to the blank group. Adapted from [124], copyright 2022, Wiley-VCH.

7. Summary and Perspective

AIEgen-based nanomaterials further enhance the antimicrobial effectiveness of AIEgens with the introduction of other materials and the construction of nanoplatfroms while retaining the advantages of AIEgens. In this review, novel antimicrobial nanomaterials constructed from AIEgens with polymers, antibiotics, metal elements, peptides, and some other materials in recent years are presented along with some of the antimicrobial strategies involved. Finally, the types, sterilization methods, mechanisms, and application scenarios of nanomaterials in different systems are summarized in Table 1.

Although these novel antimicrobial nanomaterials have made good progress in the field of antimicrobial activity, there are still some challenges and issues to be further investigated. One such issue is finding out how to further simplify the functionalised modification steps of AIEgens and how to enhance the diversity of functionalised modifications to meet the needs of a wider range of environments. A second challenge is to discover how to make greater use of the advantages of AIEgen fluorescence imaging, how to apply it to the enhancement of antibacterial performance, and how to reflect its superiority to traditional antibiotics. In addition, there is the issue of how to resolve the difficulty in reaching infected areas via laser in deep tissue phototherapy. Finally, the biocompatibility of various nanomaterials in clinical treatment and the issues related to in vivo retention and metabolism need further validation. It is hoped that this review will inspire some inspiration for researchers to do more excellent work and advance further research in this field.

Table 1. Summary of the current progress of AIEgen-based nanomaterials for bacterial imaging, detection, and therapy.

Serial Number	Type of Nanomaterial	Protocol	Application	Reference
1	Nanoparticle of polymer-based NIR-II AIEgens (PDTPBT)	NIR-II imaging-guided PTT	Subcutaneous abscess and diabetic skin infection	[60]
2	Polymeric antimicrobial cationer-based AIEgens	Electrostatic interaction	Biodegradable antibacterial agents and bacterial detection	[62]
3	Zwitterionic polymer nanoparticle-based AIEgens	Inactivation of bacteria by generating ROS under acidic conditions	Antibacterial under acidic infection sites	[112]
4	AIE nanoparticle by self-assembly	PTT and PDT of pathogens by producing $^1\text{O}_2$ and heat	Accelerate <i>S. aureus</i> -infected wound healing	[125]
5	Nanomaterial based on MSNs loading AMO, PGEDA, and TPE-(COOH) ₄	Bacterial imaging and antibacterial action with TPE-(COOH) ₄ and release of AMO	Antibacterial and bacterial detection	[126]
6	Nanoparticles with loading ciprofloxacin and AIEgens	Accurate delivery of antibiotics and dynamic monitoring	Intracellular bacterial infection	[73]
7	Organosilica nanoparticles loading rifampicin and NIR AIEgens	Imaging-guided synergistic photodynamic/antibiotic therapy	Bacterial imaging and killing	[77]
8	Ciprofloxacin-based nanodrugs with AIE	Bacterial imaging and antibacterial action with AIE-active luminogens and drugs	Combating drug-resistant bacterial infections	[127]
9	AIE-active probe based antimicrobial peptide (AMPs)	Real-time monitoring bactericidal process	Investigation of the bactericidal mechanism of AMPs	[98]
10	AIEgen-peptide-based fluorescent bioprobe specific to caspase-1	Caspase-1 activation and bacteria killing with ROS	Detection and elimination of intracellular bacteria	[90]
11	Human defensin-6 mimic peptide (HDMP) based AIEgens	Bacteria are trapped by fibrous networks and monitoring	MRSA-induced bacteraemia	[95]
12	MIL-100 (Fe) nanoparticles loading D-AzAla	Bacteria metabolic labelling and precise bacteria killing with PD	Precise bacterial detection and therapy	[98]
13	Conjugating gold nanoclusters and daptomycin	Destroy the bacterial membrane and DNA with daptomycin and ROS	MDR bacterial infection	[104]
14	A tetraphenylethylene-based discrete organoplatinum (II) metallacycle	Photodynamic inactivation with ROS generation and strong membrane-intercalating ability	Control of bacterial infections, especially for Gram-negative bacteria	[128]
15	AIE bioconjugate-based phage	Specifically targets, infects, and kills bacteria via phages and ROS	Antibiotic-sensitive and MDR bacteria-infected wounds	[113]
16	AIEgen intercalated nanoclay-based	Photodynamic/chemodynamic theranostics by generating $^1\text{O}_2$ and $\bullet\text{OH}$	<i>P. aeruginosa</i> -infected subcutaneous wounds	[81]
17	Peptide-engineered AIE nanofibers	Synergistic antibacterial activities of the ROS and peptides	Precise adjustment of antibacterial activities and bacterially infected wound healing	[124]
18	AIEgen-loaded nanofibrous membrane	Sunlight-triggered photodynamic/photothermal antipathogen	Interception of pathogenic droplets and aerosols	[129]
19	Nanoparticles-based nanographene oxide and AIEgen	Photothermal/photodynamic synergistic antibacterial	Bacterial tracer and killer	[130]

Author Contributions: Z.S.: Conceptualisation, Formal Analysis, Writing—Original Draft; Y.P.: Writing—Review and Editing; D.Y.: Supervision, Resources; D.W.: Conceptualization, Supervision, Writing—Review and Editing; B.Z.T.: Conceptualization, Supervision, Writing—Review and Editing. All authors have read and agreed to the published version of the manuscript.

Funding: This work was financially supported by the National Natural Science Foundation of China (52122317, 22175120), the Developmental Fund for Science and Technology of Shenzhen Government (JCYJ20190808153415062, RCYX20200714114525101), and the Natural Science Foundation for Distinguished Young Scholars of Guangdong Province (2020B1515020011).

Institutional Review Board Statement: Not applicable.

Informed Consent Statement: Not applicable.

Data Availability Statement: Not applicable.

Conflicts of Interest: The authors declare that they have no conflict of interest.

References

1. Hetrick, E.M.; Schoenfisch, M.H. Reducing implant-related infections: Active release strategies. *Chem. Soc. Rev.* **2006**, *35*, 780–789. [[CrossRef](#)] [[PubMed](#)]
2. Rello, J.; Campogiani, L.; Eshwara, V.K. Understanding resistance in enterococcal infections. *Intensive Care Med.* **2020**, *46*, 353–356. [[CrossRef](#)] [[PubMed](#)]
3. Liu, Y.; Shi, L.; Su, L.; van der Mei, H.C.; Jutte, P.C.; Ren, Y.; Busscher, H.J. Nanotechnology-based antimicrobials and delivery systems for biofilm-infection control. *Chem. Soc. Rev.* **2019**, *48*, 428–446. [[CrossRef](#)] [[PubMed](#)]
4. Linder, K.A.; Malani, P.N. Meningococcal Meningitis. *JAMA* **2019**, *321*, 1014. [[CrossRef](#)]
5. Fleming, A. On the antibacterial action of cultures of a penicillium, with special reference to their use in the isolation of *B. influenzae*. *Br. J. Exp. Pathol.* **1929**, *10*, 226. [[CrossRef](#)]
6. Kardas, P.; Devine, S.; Golembesky, A.; Roberts, C. A systematic review and meta-analysis of misuse of antibiotic therapies in the community. *Int. J. Antimicrob. Agents* **2005**, *26*, 106–113. [[CrossRef](#)]
7. Alanis, A.J. Resistance to Antibiotics: Are We in the Post-Antibiotic Era? *Arch. Med. Res.* **2005**, *36*, 697–705. [[CrossRef](#)]
8. Yoshikawa, T.T. Antimicrobial Resistance and Aging: Beginning of the End of the Antibiotic Era? *J. Am. Geriatr. Soc.* **2002**, *50*, 226–229. [[CrossRef](#)]
9. Willyard, C. The drug-resistant bacteria that pose the greatest health threats. *Nature* **2017**, *543*, 15. [[CrossRef](#)]
10. Garland, M.; Loscher, S.; Bogyo, M. Chemical Strategies to Target Bacterial Virulence. *Chem. Rev.* **2017**, *117*, 4422–4461. [[CrossRef](#)]
11. O'Neill, J. Tackling drug-resistant infections globally: Final report and recommendations. *Nat. Rev. Drug Discov.* **2016**, *15*, 526. [[CrossRef](#)]
12. Jampilek, J.; Kralova, K. Advances in Nanostructures for Antimicrobial Therapy. *Materials* **2022**, *15*, 2388. [[CrossRef](#)] [[PubMed](#)]
13. Xu, H.; Fang, Z.; Tian, W.; Wang, Y.; Ye, Q.; Zhang, L.; Cai, J. Green Fabrication of Amphiphilic Quaternized β -Chitin Derivatives with Excellent Biocompatibility and Antibacterial Activities for Wound Healing. *Adv. Mater.* **2018**, *30*, 1801100. [[CrossRef](#)] [[PubMed](#)]
14. Rahman, M.A.; Bam, M.; Luat, E.; Jui, M.S.; Ganewatta, M.S.; Shokfai, T.; Nagarkatti, M.; Decho, A.W.; Tang, C. Macromolecular-clustered facial amphiphilic antimicrobials. *Nat. Commun.* **2018**, *9*, 5231. [[CrossRef](#)] [[PubMed](#)]
15. Gupta, A.; Landis, R.F.; Li, C.-H.; Schnurr, M.; Das, R.; Lee, Y.-W.; Yazdani, M.; Liu, Y.; Kozlova, A.; Rotello, V.M. Engineered Polymer Nanoparticles with Unprecedented Antimicrobial Efficacy and Therapeutic Indices against Multidrug-Resistant Bacteria and Biofilms. *J. Am. Chem. Soc.* **2018**, *140*, 12137–12143. [[CrossRef](#)] [[PubMed](#)]
16. Zheng, Z.; Xu, Q.; Guo, J.; Qin, J.; Mao, H.; Wang, B.; Yan, F. Structure–Antibacterial Activity Relationships of Imidazolium-Type Ionic Liquid Monomers, Poly(ionic liquids) and Poly(ionic liquid) Membranes: Effect of Alkyl Chain Length and Cations. *ACS Appl. Mater. Interfaces* **2016**, *8*, 12684–12692. [[CrossRef](#)] [[PubMed](#)]
17. Zhang, Y.; Li, D.; Tan, J.; Chang, Z.; Liu, X.; Ma, W.; Xu, Y. Near-Infrared Regulated Nanozymatic/Photothermal/Photodynamic Triple-Therapy for Combating Multidrug-Resistant Bacterial Infections via Oxygen-Vacancy Molybdenum Trioxide Nanodots. *Small* **2021**, *17*, 2005739. [[CrossRef](#)]
18. Yuan, Z.; Tao, B.; He, Y.; Mu, C.; Liu, G.; Zhang, J.; Liao, Q.; Liu, P.; Cai, K. Remote eradication of biofilm on titanium implant via near-infrared light triggered photothermal/photodynamic therapy strategy. *Biomaterials* **2019**, *223*, 119479. [[CrossRef](#)]
19. Mao, C.; Xiang, Y.; Liu, X.; Zheng, Y.; Yeung, K.W.K.; Cui, Z.; Yang, X.; Li, Z.; Liang, Y.; Zhu, S.; et al. Local Photothermal/Photodynamic Synergistic Therapy by Disrupting Bacterial Membrane to Accelerate Reactive Oxygen Species Permeation and Protein Leakage. *ACS Appl. Mater. Interfaces* **2019**, *11*, 17902–17914. [[CrossRef](#)]
20. Lee, M.M.S.; Yan, D.; Chau, J.H.C.; Park, H.; Ma, C.C.H.; Kwok, R.T.K.; Lam, J.W.Y.; Wang, D.; Tang, B.Z. Highly efficient phototheranostics of macrophage-engulfed Gram-positive bacteria using a NIR luminogen with aggregation-induced emission characteristics. *Biomaterials* **2020**, *261*, 120340. [[CrossRef](#)]

21. Kang, M.; Zhou, C.; Wu, S.; Yu, B.; Zhang, Z.; Song, N.; Lee, M.M.S.; Xu, W.; Xu, F.-J.; Wang, D.; et al. Evaluation of Structure–Function Relationships of Aggregation-Induced Emission Luminogens for Simultaneous Dual Applications of Specific Discrimination and Efficient Photodynamic Killing of Gram-Positive Bacteria. *J. Am. Chem. Soc.* **2019**, *141*, 16781–16789. [[CrossRef](#)] [[PubMed](#)]
22. Li, Y.; Zhao, Z.; Zhang, J.; Kwok, R.T.K.; Xie, S.; Tang, R.; Jia, Y.; Yang, J.; Wang, L.; Lam, J.W.Y.; et al. A Bifunctional Aggregation-Induced Emission Luminogen for Monitoring and Killing of Multidrug-Resistant Bacteria. *Adv. Funct. Mater.* **2018**, *28*, 1804632. [[CrossRef](#)]
23. Deng, Y.; Jia, F.; Chen, S.; Shen, Z.; Jin, Q.; Fu, G.; Ji, J. Nitric oxide as an all-rounder for enhanced photodynamic therapy: Hypoxia relief, glutathione depletion and reactive nitrogen species generation. *Biomaterials* **2018**, *187*, 55–65. [[CrossRef](#)]
24. Xi, Y.; Wang, Y.; Gao, J.; Xiao, Y.; Du, J. Dual Corona Vesicles with Intrinsic Antibacterial and Enhanced Antibiotic Delivery Capabilities for Effective Treatment of Biofilm-Induced Periodontitis. *ACS Nano* **2019**, *13*, 13645–13657. [[CrossRef](#)]
25. Chu, L.; Gao, H.; Cheng, T.; Zhang, Y.; Liu, J.; Huang, F.; Yang, C.; Shi, L.; Liu, J. A charge-adaptive nanosystem for prolonged and enhanced in vivo antibiotic delivery. *Chem. Commun.* **2016**, *52*, 6265–6268. [[CrossRef](#)] [[PubMed](#)]
26. Radovic-Moreno, A.F.; Lu, T.K.; Puscasu, V.A.; Yoon, C.J.; Langer, R.; Farokhzad, O.C. Surface Charge-Switching Polymeric Nanoparticles for Bacterial Cell Wall-Targeted Delivery of Antibiotics. *ACS Nano* **2012**, *6*, 4279–4287. [[CrossRef](#)]
27. Makabenta, J.M.V.; Nabawy, A.; Li, C.-H.; Schmidt-Malan, S.; Patel, R.; Rotello, V.M. Nanomaterial-based therapeutics for antibiotic-resistant bacterial infections. *Nat. Rev. Microbiol.* **2021**, *19*, 23–36. [[CrossRef](#)]
28. Borjihan, Q.; Wu, H.; Dong, A.; Gao, H.; Yang, Y.-W. AIEgens for Bacterial Imaging and Ablation. *Adv. Healthcare Mater.* **2021**, *10*, 2100877. [[CrossRef](#)]
29. Chen, X.; Han, H.; Tang, Z.; Jin, Q.; Ji, J. Aggregation-Induced Emission-Based Platforms for the Treatment of Bacteria, Fungi, and Viruses. *Adv. Healthcare Mater.* **2021**, *10*, 2100736. [[CrossRef](#)] [[PubMed](#)]
30. Bai, H.; He, W.; Chau, J.H.C.; Zheng, Z.; Kwok, R.T.K.; Lam, J.W.Y.; Tang, B.Z. AIEgens for microbial detection and antimicrobial therapy. *Biomaterials* **2021**, *268*, 120598. [[CrossRef](#)]
31. Zhao, Z.; Chen, C.; Wu, W.; Wang, F.; Du, L.; Zhang, X.; Xiong, Y.; He, X.; Cai, Y.; Kwok, R.T.K.; et al. Highly efficient photothermal nanoagent achieved by harvesting energy via excited-state intramolecular motion within nanoparticles. *Nat. Commun.* **2019**, *10*, 768. [[CrossRef](#)] [[PubMed](#)]
32. Zhang, J.; Wang, Q.; Guo, Z.; Zhang, S.; Yan, C.; Tian, H.; Zhu, W.-H. High-Fidelity Trapping of Spatial–Temporal Mitochondria with Rational Design of Aggregation-Induced Emission Probes. *Adv. Funct. Mater.* **2019**, *29*, 1808153. [[CrossRef](#)]
33. Xie, S.; Wong, A.Y.H.; Kwok, R.T.K.; Li, Y.; Su, H.; Lam, J.W.Y.; Chen, S.; Tang, B.Z. Fluorogenic Ag⁺–Tetrazolate Aggregation Enables Efficient Fluorescent Biological Silver Staining. *Angew. Chem. Int. Ed.* **2018**, *57*, 5750–5753. [[CrossRef](#)] [[PubMed](#)]
34. Shao, A.; Xie, Y.; Zhu, S.; Guo, Z.; Zhu, S.; Guo, J.; Shi, P.; James, T.D.; Tian, H.; Zhu, W.-H. Far-Red and Near-IR AIE-Active Fluorescent Organic Nanoprobes with Enhanced Tumor-Targeting Efficacy: Shape-Specific Effects. *Angew. Chem. Int. Ed.* **2015**, *54*, 7275–7280. [[CrossRef](#)]
35. Mei, J.; Leung, N.L.C.; Kwok, R.T.K.; Lam, J.W.Y.; Tang, B.Z. Aggregation-Induced Emission: Together We Shine, United We Soar! *Chem. Rev.* **2015**, *115*, 11718–11940. [[CrossRef](#)]
36. Schulze, H.; Barl, T.; Vase, H.; Baier, S.; Thomas, P.; Giraud, G.; Crain, J.; Bachmann, T.T. Enzymatic on-Chip Enhancement for High Resolution Genotyping DNA Microarrays. *Anal. Chem.* **2012**, *84*, 5080–5084. [[CrossRef](#)]
37. Delehanty, J.B.; Ligler, F.S. A Microarray Immunoassay for Simultaneous Detection of Proteins and Bacteria. *Anal. Chem.* **2002**, *74*, 5681–5687. [[CrossRef](#)]
38. Hamid, A.M.; Jarmusch, A.K.; Pirro, V.; Pincus, D.H.; Clay, B.G.; Gervasi, G.; Cooks, R.G. Rapid Discrimination of Bacteria by Paper Spray Mass Spectrometry. *Anal. Chem.* **2014**, *86*, 7500–7507. [[CrossRef](#)]
39. Boardman, A.K.; Wong, W.S.; Premasiri, W.R.; Ziegler, L.D.; Lee, J.C.; Miljkovic, M.; Klapperich, C.M.; Sharon, A.; Sauer-Budge, A.F. Rapid Detection of Bacteria from Blood with Surface-Enhanced Raman Spectroscopy. *Anal. Chem.* **2016**, *88*, 8026–8035. [[CrossRef](#)]
40. Loman, N.J.; Misra, R.V.; Dallman, T.J.; Constantinidou, C.; Gharbia, S.E.; Wain, J.; Pallen, M.J. Performance comparison of benchtop high-throughput sequencing platforms. *Nat. Biotechnol.* **2012**, *30*, 434–439. [[CrossRef](#)]
41. Song, N.; Zhang, Z.; Liu, P.; Yang, Y.-W.; Wang, L.; Wang, D.; Tang, B.Z. Nanomaterials with Supramolecular Assembly Based on AIE Luminogens for Theranostic Applications. *Adv. Mater.* **2020**, *32*, 2004208. [[CrossRef](#)]
42. Xu, W.; Wang, D.; Tang, B.Z. NIR-II AIEgens: A Win-Win Integration towards Bioapplications. *Angew. Chem. Int. Ed.* **2021**, *60*, 7476–7487. [[CrossRef](#)] [[PubMed](#)]
43. Luo, J.; Xie, Z.; Lam, J.W.; Cheng, L.; Chen, H.; Qiu, C.; Kwok, H.S.; Zhan, X.; Liu, Y.; Zhu, D.; et al. Aggregation-induced emission of 1-methyl-1, 2, 3, 4, 5-pentaphenylsilole. *Chem. Commun.* **2001**, *18*, 1740–1741. [[CrossRef](#)] [[PubMed](#)]
44. Gao, H.; Zhang, X.; Chen, C.; Li, K.; Ding, D. Unity Makes Strength: How Aggregation-Induced Emission Luminogens Advance the Biomedical Field. *Adv. Biosyst.* **2018**, *2*, 1800074. [[CrossRef](#)]
45. Yu, Y.; Feng, C.; Hong, Y.; Liu, J.; Chen, S.; Ng, K.M.; Luo, K.Q.; Tang, B.Z. Cytophilic Fluorescent Bioprobes for Long-Term Cell Tracking. *Adv. Mater.* **2011**, *23*, 3298–3302. [[CrossRef](#)]
46. Yan, D.; Xie, W.; Zhang, J.; Wang, L.; Wang, D.; Tang, B.Z. Donor/ π -Bridge Manipulation for Constructing a Stable NIR-II Aggregation-Induced Emission Luminogen with Balanced Photo-theranostic Performance. *Angew. Chem. Int. Ed.* **2021**, *60*, 26769–26776. [[CrossRef](#)] [[PubMed](#)]

47. Song, S.; Wang, Y.; Zhao, Y.; Huang, W.; Zhang, F.; Zhu, S.; Wu, Q.; Fu, S.; Tang, B.Z.; Wang, D. Molecular Engineering of AIE Luminogens for NIR-II/IIb Bioimaging and Surgical Navigation of Lymph Nodes. *Matter* **2022**, *5*, 2847–2863. [[CrossRef](#)]
48. Qin, Y.; Chen, X.; Gui, Y.; Wang, H.; Tang, B.Z.; Wang, D. A Self-Assembled Metallacage with Second Near-Infrared Aggregation-Induced Emission for Enhanced Multimodal Theranostics. *J. Am. Chem. Soc.* **2022**, *144*, 12825–12833. [[CrossRef](#)]
49. Wang, B.; Wang, M.; Mikhailovsky, A.; Wang, S.; Bazan, G.C. A Membrane-Intercalating Conjugated Oligoelectrolyte with High-Efficiency Photodynamic Antimicrobial Activity. *Angew. Chem. Int. Ed.* **2017**, *56*, 5031–5034. [[CrossRef](#)]
50. Yan, D.; Wang, M.; Wu, Q.; Niu, N.; Li, M.; Song, R.; Rao, J.; Kang, M.; Zhang, Z.; Zhou, F.; et al. Multimodal Imaging-Guided Photothermal Immunotherapy Based on a Versatile NIR-II Aggregation-Induced Emission Luminogen. *Angew. Chem. Int. Ed.* **2022**, *61*, e202202614. [[CrossRef](#)]
51. Wang, M.; Yan, D.; Wang, M.; Wu, Q.; Song, R.; Huang, Y.; Rao, J.; Wang, D.; Zhou, F.; Tang, B.Z. A Versatile 980 nm Absorbing Aggregation-Induced Emission Luminogen for NIR-II Imaging-Guided Synergistic Photo-Immunotherapy Against Advanced Pancreatic Cancer. *Adv. Funct. Mater.* **2022**, *32*, 2205371. [[CrossRef](#)]
52. Boman, H.G. Antibacterial peptides: Key components needed in immunity. *Cell* **1991**, *65*, 205–207. [[CrossRef](#)] [[PubMed](#)]
53. Shi, X.J.; Sung, S.H.P.; Chau, J.H.C.; Li, Y.; Liu, Z.Y.; Kwok, R.T.K.; Liu, J.K.; Xiao, P.H.; Zhang, J.J.; Liu, B.; et al. Killing G(+) or G(-) Bacteria? The Important Role of Molecular Charge in AIE-Active Photosensitizers. *Small Methods* **2020**, *4*, 2000046. [[CrossRef](#)]
54. Liao, Y.; Li, B.; Zhao, Z.; Fu, Y.; Tan, Q.; Li, X.; Wang, W.; Yin, J.; Shan, H.; Tang, B.Z.; et al. Targeted Theranostics for Tuberculosis: A Rifampicin-Loaded Aggregation-Induced Emission Carrier for Granulomas Tracking and Anti-Infection. *ACS Nano* **2020**, *14*, 8046–8058. [[CrossRef](#)]
55. Chen, H.; Li, S.; Wu, M.; Kenry; Huang, Z.; Lee, C.-S.; Liu, B. Membrane-Anchoring Photosensitizer with Aggregation-Induced Emission Characteristics for Combating Multidrug-Resistant Bacteria. *Angew. Chem. Int. Ed.* **2020**, *59*, 632–636. [[CrossRef](#)]
56. Ying, M.; Zhuang, J.; Wei, X.; Zhang, X.; Zhang, Y.; Jiang, Y.; Dehaini, D.; Chen, M.; Gu, S.; Gao, W.; et al. Remote-Loaded Platelet Vesicles for Disease-Targeted Delivery of Therapeutics. *Adv. Funct. Mater.* **2018**, *28*, 1801032. [[CrossRef](#)]
57. Feng, G.; Yuan, Y.; Fang, H.; Zhang, R.; Xing, B.; Zhang, G.; Zhang, D.; Liu, B. A light-up probe with aggregation-induced emission characteristics (AIE) for selective imaging, naked-eye detection and photodynamic killing of Gram-positive bacteria. *Chem. Commun.* **2015**, *51*, 12490–12493. [[CrossRef](#)]
58. Song, W.; Zhang, Y.; Yu, D.-G.; Tran, C.H.; Wang, M.; Varyambath, A.; Kim, J.; Kim, I. Efficient Synthesis of Folate-Conjugated Hollow Polymeric Capsules for Accurate Drug Delivery to Cancer Cells. *Biomacromolecules* **2021**, *22*, 732–742. [[CrossRef](#)]
59. Song, W.; Zhang, M.; Huang, X.; Chen, B.; Ding, Y.; Zhang, Y.; Yu, D.G.; Kim, I. Smart l-borneol-loaded hierarchical hollow polymer nanospheres with antipollution and antibacterial capabilities. *Mater. Today Chem.* **2022**, *26*, 101252. [[CrossRef](#)]
60. Huang, Y.; Li, D.; Wang, D.; Chen, X.; Ferreira, L.; Martins, M.C.L.; Wang, Y.; Jin, Q.; Wang, D.; Tang, B.Z.; et al. A NIR-II emissive polymer AIEgen for imaging-guided photothermal elimination of bacterial infection. *Biomaterials* **2022**, *286*, 121579. [[CrossRef](#)]
61. Krumm, C.; Harmuth, S.; Hijazi, M.; Neugebauer, B.; Kampmann, A.-L.; Geltenpoth, H.; Sickmann, A.; Tiller, J.C. Antimicrobial Poly(2-methyloxazoline)s with Bioswitchable Activity through Satellite Group Modification. *Angew. Chem. Int. Ed.* **2014**, *53*, 3830–3834. [[CrossRef](#)] [[PubMed](#)]
62. Chen, S.; Chen, Q.; Li, Q.; An, J.; Sun, P.; Ma, J.; Gao, H. Biodegradable Synthetic Antimicrobial with Aggregation-Induced Emissive Luminogens for Temporal Antibacterial Activity and Facile Bacteria Detection. *Chem. Mater.* **2018**, *30*, 1782–1790. [[CrossRef](#)]
63. Nolivos, S.; Cayron, J.; Dedieu, A.; Page, A.; Delolme, F.; Lesterlin, C. Role of AcrAB-TolC multidrug efflux pump in drug-resistance acquisition by plasmid transfer. *Science* **2019**, *364*, 778–782. [[CrossRef](#)]
64. Spellberg, B.; Gidycz, R.; Gilbert, D.; Bradley, J.; Boucher, H.W.; Scheld, W.M.; Bartlett, J.G.; Edwards, J., Jr.; The Infectious Diseases Society of America. The Epidemic of Antibiotic-Resistant Infections: A Call to Action for the Medical Community from the Infectious Diseases Society of America. *Clin. Infect. Dis.* **2008**, *46*, 155–164. [[CrossRef](#)] [[PubMed](#)]
65. Ding, X.; Wang, A.; Tong, W.; Xu, F.-J. Biodegradable Antibacterial Polymeric Nanosystems: A New Hope to Cope with Multidrug-Resistant Bacteria. *Small* **2019**, *15*, 1900999. [[CrossRef](#)] [[PubMed](#)]
66. Armstead, A.L.; Li, B. Nanomedicine as an emerging approach against intracellular pathogens. *Int. J. Nanomed.* **2011**, *6*, 3281.
67. Abed, N.; Couvreur, P. Nanocarriers for antibiotics: A promising solution to treat intracellular bacterial infections. *Int. J. Antimicrob. Agents* **2014**, *43*, 485–496. [[CrossRef](#)]
68. Chen, H.; Jin, Y.; Wang, J.; Wang, Y.; Jiang, W.; Dai, H.; Pang, S.; Lei, L.; Ji, J.; Wang, B. Design of smart targeted and responsive drug delivery systems with enhanced antibacterial properties. *Nanoscale* **2018**, *10*, 20946–20962. [[CrossRef](#)]
69. Ji, H.; Dong, K.; Yan, Z.; Ding, C.; Chen, Z.; Ren, J.; Qu, X. Bacterial hyaluronidase self-triggered prodrug release for chemophotothermal synergistic treatment of bacterial infection. *Small* **2016**, *12*, 6200–6206. [[CrossRef](#)]
70. Xiong, M.H.; Li, Y.J.; Bao, Y.; Yang, X.Z.; Hu, B.; Wang, J. Bacteria-responsive multifunctional nanogel for targeted antibiotic delivery. *Adv. Mater.* **2012**, *24*, 6175–6180. [[CrossRef](#)]
71. Klahn, P.; Brönstrup, M. Bifunctional antimicrobial conjugates and hybrid antimicrobials. *Nat. Prod. Rep.* **2017**, *34*, 832–885. [[CrossRef](#)]
72. Skwarecki, A.S.; Milewski, S.; Schielmann, M.; Milewska, M.J. Antimicrobial molecular nanocarrier–drug conjugates. *Nanomed. Nanotechnol. Biol. Med.* **2016**, *12*, 2215–2240. [[CrossRef](#)] [[PubMed](#)]
73. Chen, M.; He, J.; Xie, S.; Wang, T.; Ran, P.; Zhang, Z.; Li, X. Intracellular bacteria destruction via traceable enzymes-responsive release and deferoxamine-mediated ingestion of antibiotics. *J. Control. Release* **2020**, *322*, 326–336. [[CrossRef](#)]

74. Yan, S.; Gao, Z.; Han, J.; Zhang, Z.; Niu, F.; Zhang, Y. Controllable fabrication of stimuli-responsive fluorescent silica nanoparticles using a tetraphenylethene-functionalized carboxylate gemini surfactant. *J. Mater. Chem. C* **2019**, *7*, 12588–12600. [[CrossRef](#)]
75. Yan, S.; Gao, Z.; Xia, Y.; Liao, X.; Han, J.; Pan, C.; Zhang, Y.; Zhai, W. Aggregation-Induced Emission Gemini Surfactant-Assisted Fabrication of Shape-Controlled Fluorescent Hollow Mesoporous Silica Nanoparticles. *Eur. J. Inorg. Chem.* **2018**, *18*, 1891–1901. [[CrossRef](#)]
76. Yan, S.; Gao, Z.; Xia, Y.; Liao, X.; Chen, Y.; Han, J.; Pan, C.; Zhang, Y. A Tetraphenylethene Luminogen-Functionalized Gemini Surfactant for Simple and Controllable Fabrication of Hollow Mesoporous Silica Nanorods with Enhanced Fluorescence. *Inorg. Chem.* **2018**, *57*, 13653–13666. [[CrossRef](#)]
77. Yan, S.; Sun, P.; Niu, N.; Zhang, Z.; Xu, W.; Zhao, S.; Wang, L.; Wang, D.; Tang, B.Z. Surfactant-Inspired Coassembly Strategy to Integrate Aggregation-Induced Emission Photosensitizer with Organosilica Nanoparticles for Efficient Theranostics. *Adv. Funct. Mater.* **2022**, *32*, 2200503. [[CrossRef](#)]
78. He, Y.; He, X. Molecular design and genetic optimization of antimicrobial peptides containing unnatural amino acids against antibiotic-resistant bacterial infections. *Peptide Sci.* **2016**, *106*, 746–756. [[CrossRef](#)]
79. Akram, A.R.; Avlonitis, N.; Lilienkampf, A.; Perez-Lopez, A.M.; McDonald, N.; Chankeshwara, S.V.; Scholefield, E.; Haslett, C.; Bradley, M.; Dhaliwal, K. A labelled-ubiquitin antimicrobial peptide for immediate in situ optical detection of live bacteria in human alveolar lung tissue. *Chem. Sci.* **2015**, *6*, 6971–6979. [[CrossRef](#)]
80. Stach, M.; Siriwardena, T.N.; Köhler, T.; van Delden, C.; Darbre, T.; Reymond, J.-L. Combining Topology and Sequence Design for the Discovery of Potent Antimicrobial Peptide Dendrimers against Multidrug-Resistant *Pseudomonas aeruginosa*. *Angew. Chem. Int. Ed.* **2014**, *53*, 12827–12831. [[CrossRef](#)]
81. Zhang, J.; Zhou, F.; He, Z.; Pan, Y.; Zhou, S.; Yan, C.; Luo, L.; Gao, Y. AIEgen Intercalated Nanoclay-Based Photodynamic/Chemodynamic Theranostic Platform for Ultra-Efficient Bacterial Eradication and Fast Wound Healing. *ACS Appl. Mater. Interfaces* **2022**, *14*, 30533–30545. [[CrossRef](#)] [[PubMed](#)]
82. Nichols, M.; Kuljanin, M.; Nategholeslam, M.; Hoang, T.; Vafaei, S.; Tomberli, B.; Gray, C.G.; DeBruin, L.; Jelokhani-Niaraki, M. Dynamic Turn Conformation of a Short Tryptophan-Rich Cationic Antimicrobial Peptide and Its Interaction with Phospholipid Membranes. *J. Phys. Chem. B* **2013**, *117*, 14697–14708. [[CrossRef](#)] [[PubMed](#)]
83. Nategholeslam, M.; Vafaei, S.; Nichols, M.; Kuljanin, M.; Jelokhani-Niaraki, M.; Tomberli, B.; Gray, C.G. Structure of the Antimicrobial Peptide HHC-36 and its Interaction with Model Cell Membranes. *Biophys. J.* **2012**, *102*, 397a–398a. [[CrossRef](#)]
84. Bunschoten, A.; Welling, M.M.; Termaat, M.F.; Sathekge, M.; van Leeuwen, F.W.B. Development and Prospects of Dedicated Tracers for the Molecular Imaging of Bacterial Infections. *Bioconj. Chem.* **2013**, *24*, 1971–1989. [[CrossRef](#)]
85. Hartmann, M.; Berditsch, M.; Hawecker, J.; Ardakani, M.F.; Gerthsen, D.; Ulrich, A.S. Damage of the Bacterial Cell Envelope by Antimicrobial Peptides Gramicidin S and PGLa as Revealed by Transmission and Scanning Electron Microscopy. *Antimicrob. Agents Chemother.* **2010**, *54*, 3132–3142. [[CrossRef](#)]
86. Anderson, R.C.; Haverkamp, R.G.; Yu, P.-L. Investigation of morphological changes to *Staphylococcus aureus* induced by ovine-derived antimicrobial peptides using TEM and AFM. *FEMS Microbiol. Lett.* **2004**, *240*, 105–110. [[CrossRef](#)]
87. Rajasekhar, K.; Narayanaswamy, N.; Murugan, N.A.; Kuang, G.; Ågren, H.; Govindaraju, T. A High Affinity Red Fluorescence and Colorimetric Probe for Amyloid β Aggregates. *Sci. Rep.* **2016**, *6*, 23668. [[CrossRef](#)] [[PubMed](#)]
88. Jameson, L.P.; Smith, N.W.; Dzyuba, S.V. Dye-binding assays for evaluation of the effects of small molecule inhibitors on amyloid (A β) self-assembly. *ACS Chem. Neurosci.* **2012**, *3*, 807–819. [[CrossRef](#)]
89. Chen, J.; Gao, M.; Wang, L.; Li, S.; He, J.; Qin, A.; Ren, L.; Wang, Y.; Tang, B.Z. Aggregation-Induced Emission Probe for Study of the Bactericidal Mechanism of Antimicrobial Peptides. *ACS Appl. Mater. Interfaces* **2018**, *10*, 11436–11442. [[CrossRef](#)]
90. Qi, G.; Hu, F.; Kenry; Shi, L.; Wu, M.; Liu, B. An AIEgen-Peptide Conjugate as a Phototheranostic Agent for Phagosome-Entrapped Bacteria. *Angew. Chem. Int. Ed.* **2019**, *58*, 16229–16235. [[CrossRef](#)]
91. Nicholson, J.K.; Holmes, E.; Kinross, J.; Burcelin, R.; Gibson, G.; Jia, W.; Pettersson, S. Host-Gut Microbiota Metabolic Interactions. *Science* **2012**, *336*, 1262–1267. [[CrossRef](#)] [[PubMed](#)]
92. Horcajada, P.; Serre, C.; Vallet-Regí, M.; Sebban, M.; Taulelle, F.; Férey, G. Metal–Organic Frameworks as Efficient Materials for Drug Delivery. *Angew. Chem. Int. Ed.* **2006**, *118*, 6120–6124. [[CrossRef](#)]
93. Ayabe, T.; Satchell, D.P.; Wilson, C.L.; Parks, W.C.; Selsted, M.E.; Ouellette, A.J. Secretion of microbicidal α -defensins by intestinal Paneth cells in response to bacteria. *Nat. Immunol.* **2000**, *1*, 113–118. [[CrossRef](#)] [[PubMed](#)]
94. Chairatana, P.; Nolan, E.M. Molecular Basis for Self-Assembly of a Human Host-Defense Peptide That Entraps Bacterial Pathogens. *J. Am. Chem. Soc.* **2014**, *136*, 13267–13276. [[CrossRef](#)] [[PubMed](#)]
95. Fan, Y.; Li, X.-D.; He, P.-P.; Hu, X.-X.; Zhang, K.; Fan, J.-Q.; Yang, P.-P.; Zheng, H.-Y.; Tian, W.; Chen, Z.-M.; et al. A biomimetic peptide recognizes and traps bacteria in vivo as human defensin-6. *Sci. Adv.* **2020**, *6*, eaaz4767. [[CrossRef](#)]
96. Abánades Lázaro, I.; Haddad, S.; Sacca, S.; Orellana-Tavra, C.; Fairen-Jimenez, D.; Forgan, R.S. Selective Surface PEGylation of UiO-66 Nanoparticles for Enhanced Stability, Cell Uptake, and pH-Responsive Drug Delivery. *Chem* **2017**, *2*, 561–578. [[CrossRef](#)]
97. Wu, M.-X.; Yang, Y.-W. Metal–Organic Framework (MOF)-Based Drug/Cargo Delivery and Cancer Therapy. *Adv. Mater.* **2017**, *29*, 1606134. [[CrossRef](#)]
98. Mao, D.; Hu, F.; Kenry; Ji, S.; Wu, W.; Ding, D.; Kong, D.; Liu, B. Metal–Organic-Framework-Assisted In Vivo Bacterial Metabolic Labeling and Precise Antibacterial Therapy. *Adv. Mater.* **2018**, *30*, 1706831. [[CrossRef](#)]

99. Zheng, Y.; Lai, L.; Liu, W.; Jiang, H.; Wang, X. Recent advances in biomedical applications of fluorescent gold nanoclusters. *Adv. Colloid Interface Sci.* **2017**, *242*, 1–16. [[CrossRef](#)]
100. Jin, R.; Zeng, C.; Zhou, M.; Chen, Y. Atomically Precise Colloidal Metal Nanoclusters and Nanoparticles: Fundamentals and Opportunities. *Chem. Rev.* **2016**, *116*, 10346–10413. [[CrossRef](#)]
101. Yang, X.; Yang, M.; Pang, B.; Vara, M.; Xia, Y. Gold Nanomaterials at Work in Biomedicine. *Chem. Rev.* **2015**, *115*, 10410–10488. [[CrossRef](#)]
102. Zheng, K.; Setyawati, M.I.; Leong, D.T.; Xie, J. Antimicrobial Gold Nanoclusters. *ACS Nano* **2017**, *11*, 6904–6910. [[CrossRef](#)] [[PubMed](#)]
103. Chen, W.-Y.; Chang, H.-Y.; Lu, J.-K.; Huang, Y.-C.; Harroun, S.G.; Tseng, Y.-T.; Li, Y.-J.; Huang, C.-C.; Chang, H.-T. Self-Assembly of Antimicrobial Peptides on Gold Nanodots: Against Multidrug-Resistant Bacteria and Wound-Healing Application. *Adv. Funct. Mater.* **2015**, *25*, 7189–7199. [[CrossRef](#)]
104. Zheng, Y.; Liu, W.; Chen, Y.; Li, C.; Jiang, H.; Wang, X. Conjugating gold nanoclusters and antimicrobial peptides: From aggregation-induced emission to antibacterial synergy. *J. Colloid Interface Sci.* **2019**, *546*, 1–10. [[CrossRef](#)] [[PubMed](#)]
105. Zheng, D.-W.; Dong, X.; Pan, P.; Chen, K.-W.; Fan, J.-X.; Cheng, S.-X.; Zhang, X.-Z. Phage-guided modulation of the gut microbiota of mouse models of colorectal cancer augments their responses to chemotherapy. *Nat. Biomed. Eng.* **2019**, *3*, 717–728. [[CrossRef](#)] [[PubMed](#)]
106. Routy, B.; Le Chatelier, E.; Derosa, L.; Duong, C.P.M.; Alou, M.T.; Daillère, R.; Fluckiger, A.; Messaoudene, M.; Rauber, C.; Roberti, M.P.; et al. Gut microbiome influences efficacy of PD-1-based immunotherapy against epithelial tumors. *Science* **2018**, *359*, 91–97. [[PubMed](#)]
107. Yu, T.; Guo, F.; Yu, Y.; Sun, T.; Ma, D.; Han, J.; Qian, Y.; Kryczek, I.; Sun, D.; Nagarsheth, N.; et al. *Fusobacterium nucleatum* Promotes Chemoresistance to Colorectal Cancer by Modulating Autophagy. *Cell* **2017**, *170*, 548–563. [[CrossRef](#)]
108. Tremaroli, V.; Bäckhed, F. Functional interactions between the gut microbiota and host metabolism. *Nature* **2012**, *489*, 242–249. [[CrossRef](#)]
109. Nobrega, F.L.; Vlot, M.; de Jonge, P.A.; Dreesens, L.L.; Beaumont, H.J.E.; Lavigne, R.; Dutilh, B.E.; Brouns, S.J.J. Targeting mechanisms of tailed bacteriophages. *Nat. Rev. Microbiol.* **2018**, *16*, 760–773. [[CrossRef](#)]
110. Brockhurst, M.A.; Morgan, A.D.; Fenton, A.; Buckling, A. Experimental coevolution with bacteria and phage: The *Pseudomonas fluorescens*- Φ 2 model system. *Infect. Genet. Evol.* **2007**, *7*, 547–552. [[CrossRef](#)]
111. Thiel, K. Old dogma, new tricks—21st Century phage therapy. *Nat. Biotechnol.* **2004**, *22*, 31–36. [[CrossRef](#)] [[PubMed](#)]
112. Zhang, Q.-G.; Buckling, A. Phages limit the evolution of bacterial antibiotic resistance in experimental microcosms. *Evol. Appl.* **2012**, *5*, 575–582. [[CrossRef](#)] [[PubMed](#)]
113. He, X.; Yang, Y.; Guo, Y.; Lu, S.; Du, Y.; Li, J.-J.; Zhang, X.; Leung, N.L.C.; Zhao, Z.; Niu, G.; et al. Phage-Guided Targeting, Discriminative Imaging, and Synergistic Killing of Bacteria by AIE Bioconjugates. *J. Am. Chem. Soc.* **2020**, *142*, 3959–3969. [[CrossRef](#)] [[PubMed](#)]
114. Pan, Y.; Gao, Y.; Hu, J.; Ye, G.; Zhou, F.; Yan, C. Montmorillonite nanosheets with enhanced photodynamic performance for synergistic bacterial ablation. *J. Mater. Chem. B* **2021**, *9*, 404–409. [[CrossRef](#)]
115. Murugesan, S.; Scheibel, T. Copolymer/Clay Nanocomposites for Biomedical Applications. *Adv. Funct. Mater.* **2020**, *30*, 1908101. [[CrossRef](#)]
116. Gozali Balkanloo, P.; Mahmoudian, M.; Hosseinzadeh, M.T. A comparative study between MMT-Fe₃O₄/PES, MMT-HBE/PES, and MMT-acid activated/PES mixed matrix membranes. *Chem. Eng. J.* **2020**, *396*, 125188. [[CrossRef](#)]
117. Hong, H.-J.; Kim, J.; Kim, D.-Y.; Kang, I.; Kang, H.K.; Ryu, B.G. Synthesis of carboxymethylated nanocellulose fabricated ciprofloxacin–Montmorillonite composite for sustained delivery of antibiotics. *Int. J. Pharm.* **2019**, *567*, 118502. [[CrossRef](#)]
118. Xu, Q.; Li, X.; Jin, Y.; Sun, L.; Ding, X.; Liang, L.; Wang, L.; Nan, K.; Ji, J.; Chen, H.; et al. Bacterial self-defense antibiotics release from organic–inorganic hybrid multilayer films for long-term anti-adhesion and biofilm inhibition properties. *Nanoscale* **2017**, *9*, 19245–19254. [[CrossRef](#)]
119. Li, Z.; Chang, P.-H.; Jiang, W.-T.; Jean, J.-S. The multi-mechanisms and interlayer configurations of metoprolol uptake on montmorillonite. *Chem. Eng. J.* **2019**, *360*, 325–333. [[CrossRef](#)]
120. Liu, J.; Wang, Y.; Fan, X.; Liu, H.; Li, J.; He, X.; Hui, A.; Wang, A. The high-efficiency synergistic and broad-spectrum antibacterial effect of cobalt doped zinc oxide quantum dots (Co-ZnO QDs) loaded cetyltributylphosphonium bromide (CTPB) modified MMT (C-MMT) nanocomposites. *Colloids Surf. Physicochem. Eng. Aspects* **2021**, *613*, 126059. [[CrossRef](#)]
121. Ma, Y.-L.; Yang, B.; Xie, L. Adsorptive property of Cu²⁺–ZnO/cetylpyridinium–montmorillonite complexes for pathogenic bacterium in vitro. *Colloids Surf. B. Biointerfaces* **2010**, *79*, 390–396. [[CrossRef](#)] [[PubMed](#)]
122. Ren, B.; Li, K.; Liu, Z.; Liu, G.; Wang, H. White light-triggered zwitterionic polymer nanoparticles based on an AIE-active photosensitizer for photodynamic antimicrobial therapy. *J. Mater. Chem. B* **2020**, *8*, 10754–10763. [[CrossRef](#)] [[PubMed](#)]
123. Mao, D.; Hu, F.; Kenry, Q.; G.; Ji, S.; Wu, W.; Kong, D.; Liu, B. One-step in vivo metabolic labeling as a theranostic approach for overcoming drug-resistant bacterial infections. *Mater. Horiz.* **2020**, *7*, 1138–1143. [[CrossRef](#)]
124. Guo, K.; Zhang, M.; Cai, J.; Ma, Z.; Fang, Z.; Zhou, H.; Chen, J.; Gao, M.; Wang, L. Peptide-Engineered AIE Nanofibers with Excellent and Precisely Adjustable Antibacterial Activity. *Small* **2022**, *18*, 2108030. [[CrossRef](#)] [[PubMed](#)]

125. Wang, W.; Wu, F.; Zhang, Q.; Zhou, N.; Zhang, M.; Zheng, T.; Li, Y.; Tang, B.Z. Aggregation-Induced Emission Nanoparticles for Single Near-Infrared Light-Triggered Photodynamic and Photothermal Antibacterial Therapy. *ACS Nano* **2022**, *16*, 7961–7970. [[CrossRef](#)] [[PubMed](#)]
126. Li, Q.; Wu, Y.; Lu, H.; Wu, X.; Chen, S.; Song, N.; Yang, Y.-W.; Gao, H. Construction of Supramolecular Nanoassembly for Responsive Bacterial Elimination and Effective Bacterial Detection. *ACS Appl. Mater. Interfaces* **2017**, *9*, 10180–10189. [[CrossRef](#)]
127. Xie, S.; Manuguri, S.; Proietti, G.; Romson, J.; Fu, Y.; Inge, A.K.; Wu, B.; Zhang, Y.; Häll, D.; Ramström, O.; et al. Design and synthesis of theranostic antibiotic nanodrugs that display enhanced antibacterial activity and luminescence. *Proc. Natl. Acad. Sci. USA* **2017**, *114*, 8464–8469. [[CrossRef](#)]
128. Gao, S.; Yan, X.; Xie, G.; Zhu, M.; Ju, X.; Stang, P.J.; Tian, Y.; Niu, Z. Membrane intercalation-enhanced photodynamic inactivation of bacteria by a metallacycle and TAT-decorated virus coat protein. *Proc. Natl. Acad. Sci. USA* **2019**, *116*, 23437–23443. [[CrossRef](#)]
129. Li, M.; Wen, H.; Li, H.; Yan, Z.-C.; Li, Y.; Wang, L.; Wang, D.; Tang, B.Z. AIEgen-loaded nanofibrous membrane as photodynamic/photothermal antimicrobial surface for sunlight-triggered bioprotection. *Biomaterials* **2021**, *276*, 121007. [[CrossRef](#)]
130. Zhang, Y.X.; Fu, H.; Liu, D.E.; An, J.X.; Gao, H. Construction of biocompatible bovine serum albumin nanoparticles composed of nano graphene oxide and AIEgen for dual-mode phototherapy bacteriostatic and bacterial tracking. *J. Nanobiotechnol.* **2019**, *17*, 12. [[CrossRef](#)]

Disclaimer/Publisher’s Note: The statements, opinions and data contained in all publications are solely those of the individual author(s) and contributor(s) and not of MDPI and/or the editor(s). MDPI and/or the editor(s) disclaim responsibility for any injury to people or property resulting from any ideas, methods, instructions or products referred to in the content.